The study on the resonance demand in benzylic solvolyses

中田, 和秀
九州大学理学研究科化学専攻

https://doi.org/10.11501/3081162

出版情報：九州大学, 1994, 博士（理学）, 課程博士
バージョン：
権利関係：

Chapter 4 Ab Initio Calculation for Some Benzylic Cations

The Yukawa-Tsuno (LArSR) equation (4-1),[1)]

$$\log (k/k_0) = \rho (\sigma^0 + r \Delta\bar{\sigma}_R^+), \qquad (4\text{-}1)$$

is one of the most useful tool to predict characters of transition state of reactions affected by benzene π-system, and was successfully applied to a wide variety of reaction systems.[2-3)] This equation is characterized by the resonance demand parameter r which indicates the degree of resonance interaction between the reaction center and benzene π-system.

In substituent effect studies on gas phase stabilities, the same r values with those in solvolysis were obtained; r=1.00 for α,α-dimethylbenzyl cations (**9**),[3f)] r=1.01 for α-ethyl-α-methylbenzyl cations (**10**),[3e)] r=1.14 for α-methylbenzyl cations (**4**),[3d)] r=1.29 for benzyl cations (**3**),[3c)] r=1.41 for α-methyl-α-trifluoromethylbenzyl cations (**2**),[3b)] and r=1.54 for α-trifluoromethylbenzyl cations (**1**).[3a)] This shows that the resonance structures of the transition state in S_N1 solvolysis and corresponding cation are very similar. Moreover, in case of α-*t*-butyl-α-methylbenzyl cation (**14**), identical r value of 0.86[3g)] with that of the corresponding solvolysis (r=0.91)[2i)] was obtained, suggesting the twisted structure of the transition state of benzylic solvolysis remains unchanged from the deviation from coplanarity of the related cation. Thus one can use cation as a model of transition state of S_N1 solvolysis. As discussed in

chapter 3, good relation between the r value and the intrinsic stability of the parent cation exists as far as the benzene π-orbital and a vacant p-orbital lie on the same plane. This suggests that the unsubstituted benzylic cations are very important species to interpret the r value theoretically.

In organic chemistry, the "resonance theory" which is derived from valence bond theory is of course important concept to predict reactivity. This theory estimates changes of physical constants (stabilization energy, bond length, charge density, bond order, and so on) qualitatively, which is affected by resonance. Thus the existence of good correlation between the r values and physical quantities of benzylic cations which is calculated by molecular orbital theory provides the real origin of the r value.

From this point of view, the geometries of parent benzylic cations were optimized by ab initio MO methods using several different levels of basis sets.

Method

The ab initio LCAO-MO method[4] was used for the study of α-substituted benzyl cations: α-trifluoromethylbenzyl cation (**1**), α-trifluoromethyl-α-methylbenzyl cation (**2**), benzyl cation (**3**), α-methylbenzyl cation (**4**), 2,2-dimethyl-1-indanyl cation (**5**), α-*t*-butylbenzyl cation (**6**), α-*t*-butyl-*o*-methylbenzyl cation (**7**), α-*t*-butyl-*o*,*o*-dimethylbenzyl cation (**8**), α,α-dimethylbenzyl cation (**9**), α-ethyl-α-methylbenzyl cation (**10**), α,α-diethylbenzyl cation

(**11**) α-isopropyl-α-methylbenzyl cation (**12**), α,α-diisopropylbenzyl cation (**13**) α-*t*-butyl-α-methylbenzyl cation (**14**), α-*t*-butyl-α-isopropylbenzyl cation (**15**), α,α-di-*t*-butylbenzyl cation (**16**), 4-methylbenzobicyclo[2.2.2]octen-1-yl cation (**17**), α,α-dimethylbenzyl cation (θ=90° fixed, **18**), α-methylbenzyl cation (θ=90° fixed, **19**), benzyl cation (θ=90° fixed, **20**). Structural formulas of these cations were shown in Figs. 4-1 (**1-10**) and 4-2 (**11-20**). In order to check the free energy change in proton or chloride transfer reactions in two benzylic systems, the corresponding precursors, olefins and chlorides, are also calculated by ab initio MO method. All calculations were performed on the IBM RS/6000 computer with GAUSSIAN-92 suite of programs.[5] Geometries were optimized completely by the gradient procedure[6] at the C_1 symmetry. The closed-shell restricted Hartree-Fock level with STO-3G, 3-21G, and 6-31G* basis sets was applied to find stationary points on the potential energy surface (PES). At RHF/6-31G* level all optimized structures were checked by analysis of harmonic vibrational frequencies obtained from diagonalization of force constant matrices to find the order of the stationary points. To improve the calculated energies, electron-correlation contributions were determined by Møller-Plesset perturbation theory;[7] single-point MP2 calculations were carried out at the 6-31G* basis set using the frozen-core approximation. Such a calculation is denoted MP2/6-31G*//RHF/6-31G*, where // means "at the geometry of". The relative final energies were corrected for RHF/6-31G* zero-point energy (ZPE) differences scaled by the factor

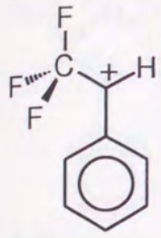

1a
α-trifluoro-
methylbenzyl
cation.

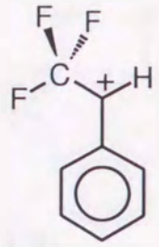

1b
α-trifluoro-
methylbenzyl
cation.

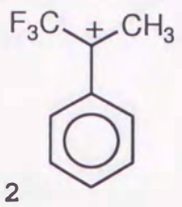

2
α-trifluoro-
methyl-α-
methylbenzyl
cation.

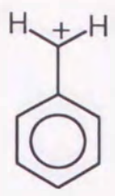

3
benzyl
cation.

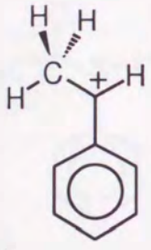

4a
α-methyl-
benzyl cation.

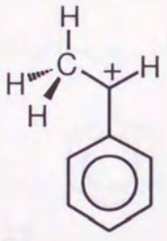

4b
α-methyl-
benzyl cation.

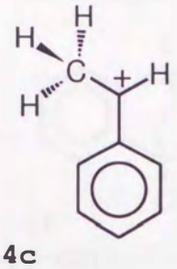

4c
α-methyl-
benzyl cation.

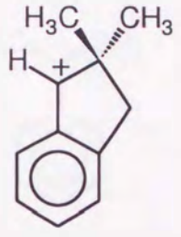

5
2,2-dimethyl-
1-indanyl
cation.

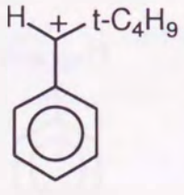

6
α-tert-butyl
benzyl cation.

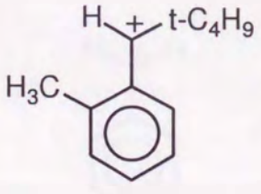

7
α-tert-butyl-
o-methyl
benzyl cation.

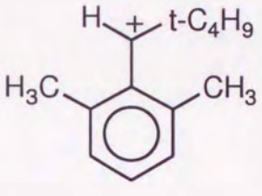

8
α-tert-butyl-
o,o-dimethyl
benzyl cation.

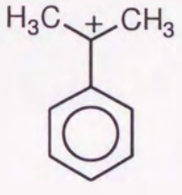

9
α,α-dimethyl-
benzyl cation.

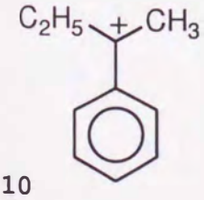

10
α-ethyl-
α-methyl
benzyl cation.

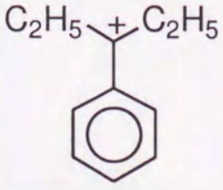

11
α,α-diethyl-
benzyl cation.

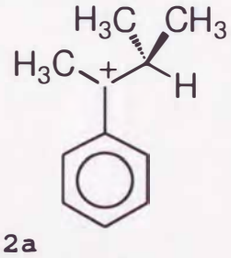

12a
α-isopropyl-
α-methylbenzyl
cation.

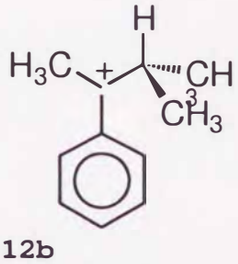

12b
α-isopropyl-
α-methylbenzyl
cation.

Fig. 4-1. Calculated benzylic cations (**1**-**12**).

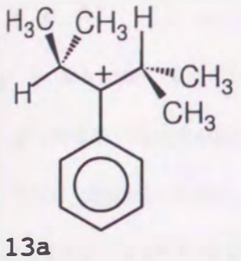

13a
α,α-diiso-
propylbenzyl
cation.

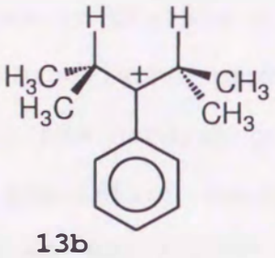

13b
α,α-diiso-
propylbenzyl
cation.

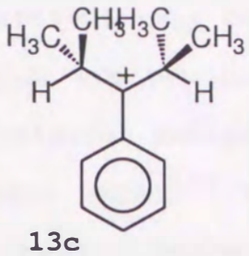

13c
α,α-diiso-
propylbenzyl
cation.

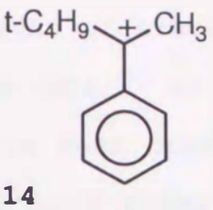

14
α-tert-butyl-
α-methylbenzyl
cation.

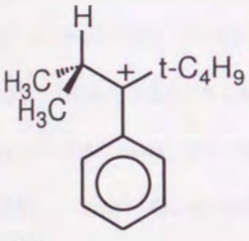

15
α-tert-butyl-
α-isopropyl-
benzyl cation.

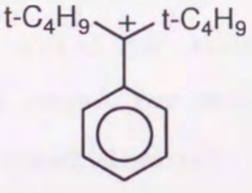

16
α,α-di-tert-
butylbenzyl
cation.

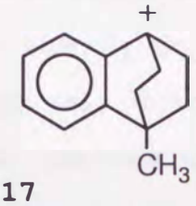

17
4-methyl-
benzobicyclo
[2.2.2]octen-
1-yl cation

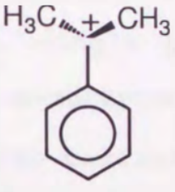

18
α,α-dimethyl-
benzyl cation
(90° fixed).

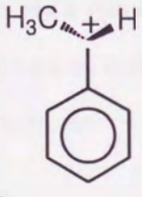

19
α-methyl-
benzyl cation
(90° fixed).

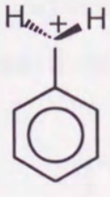

20
benzyl cation
(90° fixed).

Fig. 4-2. Calculated benzylic cations (**13-20**).

of 0.9.[8] In order to discuss quantitatively the relation between the r value in Yukawa-Tsuno equation and populations of electrons at atomic centers, the natural population analysis (NPA)[9] as well as the Mulliken population analysis (MPA)[10] have been done for benzylic cations at RHF/6-31G* level. Wieberg bond orders in natural bonding orbital (NBO)[9] analysis are also calculated to discuss the origin of the r value. In order to examine the effect of electron correlation on the torsion angle and the force constant for the hindered rotation around the C_1-C_7 axis, single point calculation at MP2 level for α-cumyl (**9**), α-*t*-butyl-α-methylbenzyl (**14**), and α,α-di-*t*-butylbenzyl (**16**) cations were also carried out with the geometry whose dihedral angle θ (shown in Fig. 4-3) changes by ±5° around the RHF/6-31G* optimized geometry. For α-methylbenzyl cations (**4a-c**) whose conformations are α-methyl rotamers one another, calculations were extended to MP2(FU)/6-31G* optimization to estimate the effect of hyperconjugation on the structure.

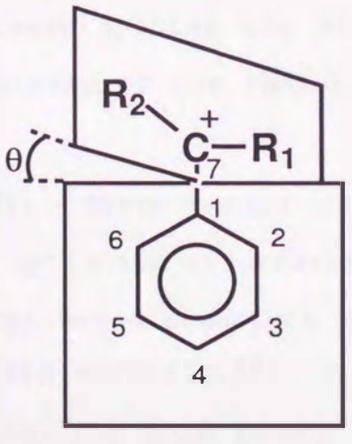

θ = (|180-∠R1C7C1C6| + |∠R2C7C1C6|)/2.

Fig. 4-3. The numbering of atoms for α-substituted benzylic cations.

Results and Discussion

Energies and Geometries. The optimized structures of benzylic cations at RHF/6-31G* are shown in Figs. 4-4 - 4-10, and their selected geometrical parameters are summarized in Tables 4-1 - 4-7. Total energies are listed in Table 4-9. The numbering of atoms and the dihedral angle θ are given in Fig. 4-3. Calculated dihedral angles of $\angle R_1C_7C_1R_2$, $\angle C_2C_1C_7C_6$, $\angle C_1C_2C_3C_4$, $\angle C_2C_3C_4C_5$, $\angle C_3C_4C_5C_6$, $\angle C_4C_5C_6C_1$, $\angle C_5C_6C_1C_2$, and $\angle C_6C_1C_2C_3$ for all benzylic cations without **8** are less than 3.0°, indicating phenyl rings are actually planar and interactions between vacant p orbital and benzene π system are π-type. Thus electronic effect of α-substituents (R_1, R_2) and dihedral angle θ are considered to real factors which determine the degree of resonance interaction for these benzylic cations. So that changes of physical quantities on aromatic moiety reflect the degree of resonance. As shown in Table 4-9, most stable conformations have only positive vibrational frequencies so that these species are minimum structures at the RHF/6-31G* PES. Geometries of the individual benzylic cation are discussed below.

Benzyl Cation (3). Since benzyl cation is the most simple benzylic cation, some optimized structures by ab initio MO method are reported.[11,12] Optimized structure with HF/6-31G* (Fig. 4-4) is agreed with that with HF/3-21G.[12] C_1-C_2 (1.436 Å) and C_3-C_4 (1.403 Å) are longer than C-C bond length of benzene (1.39 Å), and C_2-C_3 (1.362 Å) is shorter. Contributions of five resonance

Table 4-1. Selected Geometric Parameters[a] of **1a**-**3** Optimized at RHF/6-31G*.

	Cations			
	α-CF_3-benzyl (**1a**)	(**1b**)	α-CF_3-α-CH_3-benzyl (**2**)	Benzyl (**3**)
C1-C2	1.443	1.446	1.438	1.436
C2-C3	1.360	1.360	1.362	1.362
C3-C4	1.403	1.403	1.400	1.403
C4-C5	1.406	1.405	1.398	1.403
C5-C6	1.359	1.359	1.364	1.362
C6-C1	1.445	1.446	1.440	1.436
C1-C7	1.353	1.354	1.379	1.357
C7-R1[b]	1.076	1.076	1.490	1.075
C7-R2[b]	1.523	1.518	1.543	1.075
C7-C1-C2	118.2	116.7	120.8	120.4
C7-C1-C6	123.1	124.9	121.8	120.4
C1-C7-R1[b]	120.2	118.8	126.5	121.7
C1-C7-R2[b]	125.5	130.6	120.0	121.7
θ[c]	0	0	0	0

a) Distance in angstroms, angle in degrees. b) R_1 and R_2 correspond right and left atoms bonded to C_7 given in Fig. 4-4, respectively. The numbering of atom are given in Fig. 4-3. c) Mean dihedral angle of |180-∠R1C7C1C6| and |∠R2C7C1C6|.

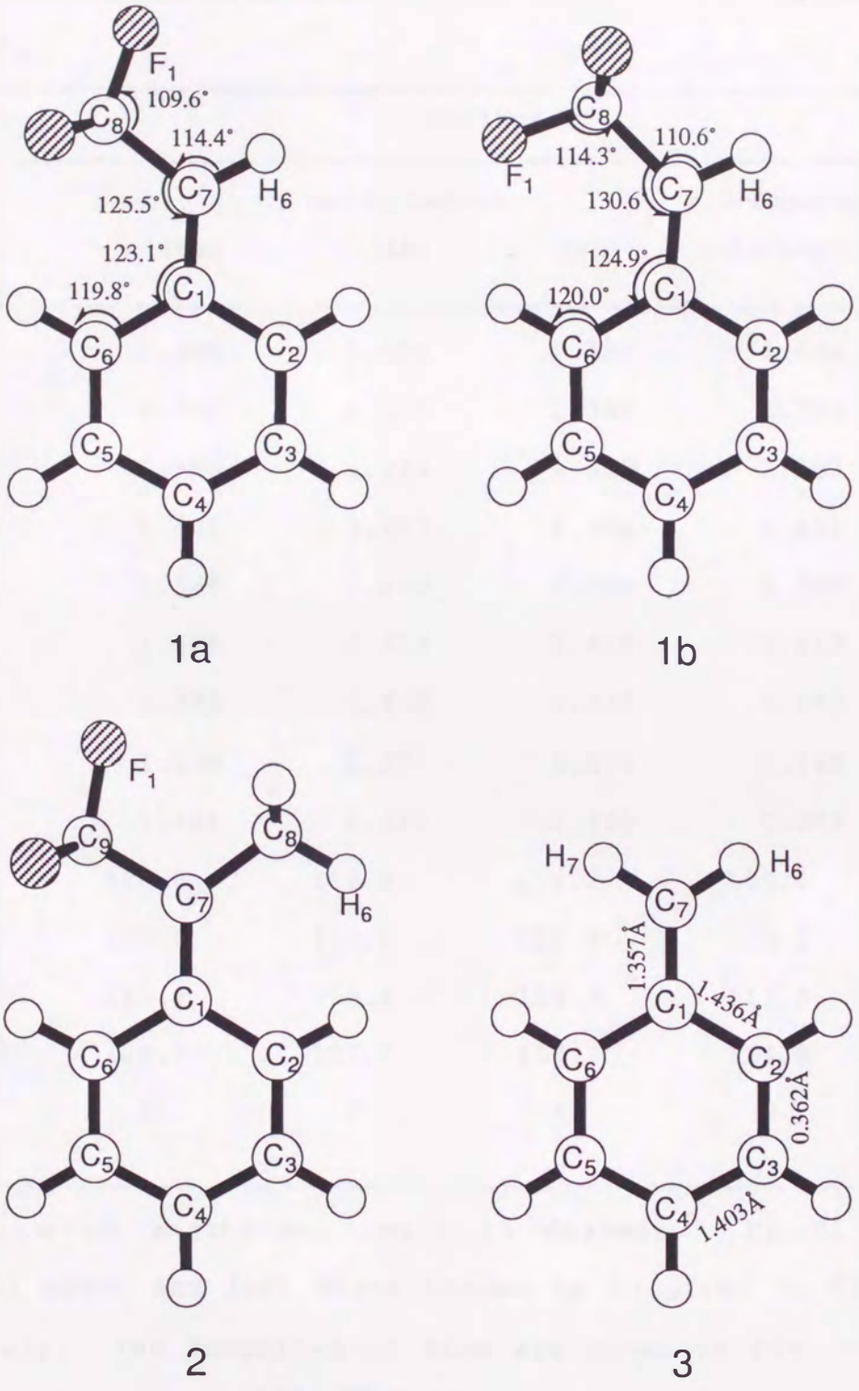

Fig. 4-4. RHF/6-31G* optimized structures of **1-3**.

Table 4-2. Selected Geometric Parameters[a] of **4a-5** Optimized at RHF/6-31G*.

	Cations			
	(**4a**)	α-CH_3-benzyl (**4b**)	(**4c**)	2,2-Dimethyl-1-indanyl (**5**)
C1-C2	1.428	1.426	1.427	1.424
C2-C3	1.368	1.369	1.368	1.374
C3-C4	1.396	1.395	1.395	1.387
C4-C5	1.402	1.403	1.402	1.411
C5-C6	1.364	1.363	1.364	1.360
C6-C1	1.429	1.429	1.429	1.419
C1-C7	1.378	1.378	1.378	1.369
C7-R1[b]	1.078	1.077	1.077	1.498
C7-R2[b]	1.481	1.490	1.484	1.074
C7-C1-C2	118.0	118.5	118.2	109.4
C7-C1-C6	123.0	122.6	122.9	129.5
C1-C7-R1[b]	116.3	116.4	116.3	113.0
C1-C7-R2[b]	129.2	127.0	128.3	124.8
θ[c]	0	0	1	0

a) Distance in angstroms, angle in degrees. b) R_1 and R_2 correspond right and left atoms bonded to C_7 given in Fig. 4-5, respectively. The numbering of atom are given in Fig. 4-3. c) Mean dihedral angle of |180-∠R1C7C1C6| and |∠R2C7C1C6|.

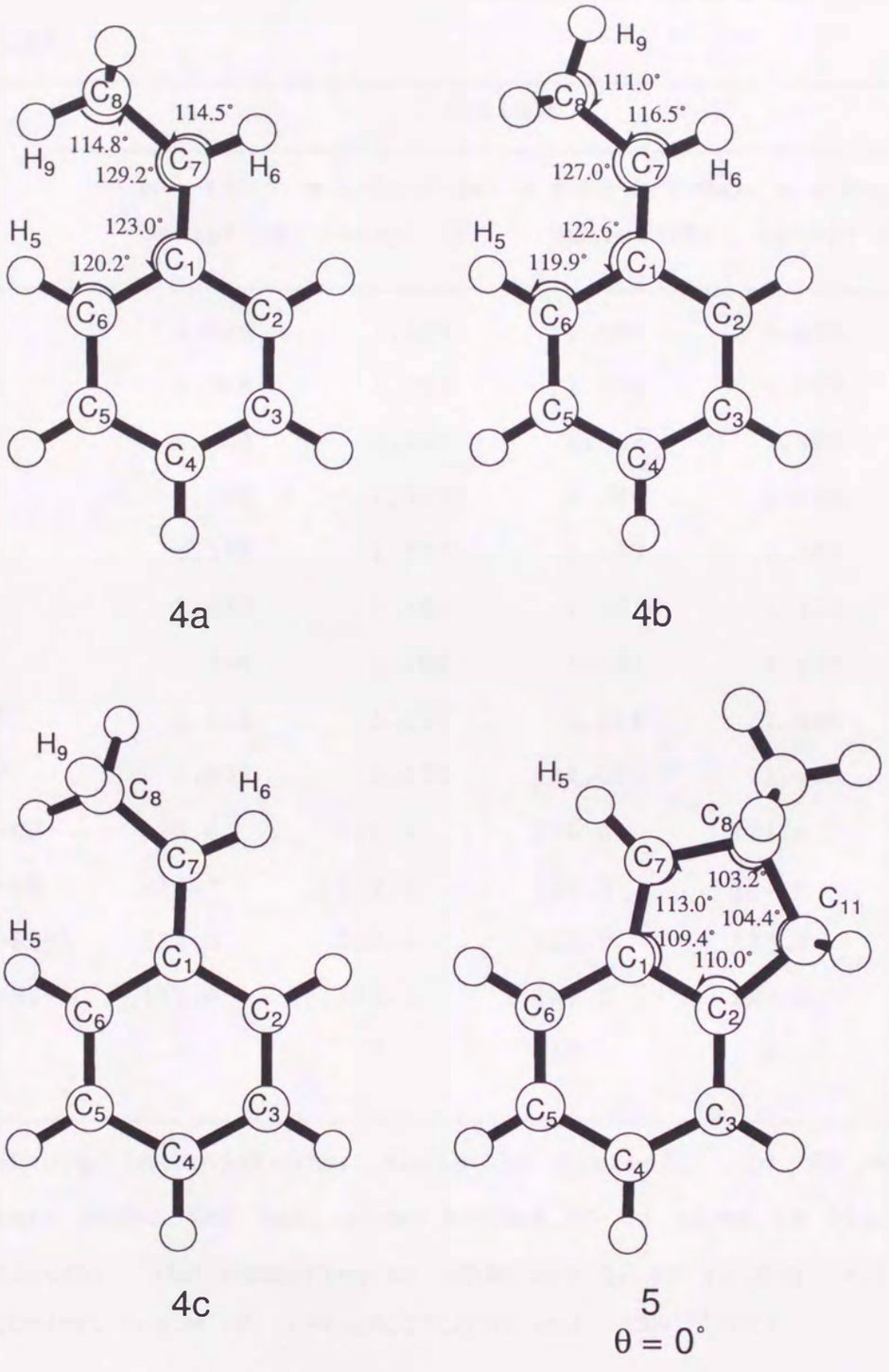

Fig. 4-5. RHF/6-31G* optimized structures of **4**-**5**.

Table 4-3. Selected Geometric Parameters[a] of **6-9** Optimized at RHF/6-31G*.

	Cations			
	α-t-Bu-benzyl (**6**)	α-t-Bu-2-Me-benzyl (**7**)	α-t-Bu-2,2-Me_2-benzyl (**8**)	α,α-Me_2-benzyl (**9**)
C1-C2	1.429	1.435	1.450	1.423
C2-C3	1.364	1.359	1.371	1.369
C3-C4	1.402	1.400	1.392	1.395
C4-C5	1.393	1.389	1.389	1.395
C5-C6	1.370	1.379	1.373	1.369
C6-C1	1.427	1.446	1.457	1.424
C1-C7	1.386	1.380	1.383	1.404
C7-R1[b]	1.511	1.517	1.514	1.496
C7-R2[b]	1.078	1.075	1.072	1.495
C7-C1-C2	125.0	122.4	126.8	121.0
C7-C1-C6	116.7	118.9	114.3	121.0
C1-C7-R1[b]	132.3	132.6	138.8	123.2
C1-C7-R2[b]	113.6	114.5	112.5	123.2
θ[c]	0	0	19	5

a) Distance in angstroms, angle in degrees. b) R_1 and R_2 correspond right and left atoms bonded to C_7 given in Fig. 4-6, respectively. The numbering of atom are given in Fig. 4-3. c) Mean dihedral angle of |180-∠R1C7C1C6| and |∠R2C7C1C6|.

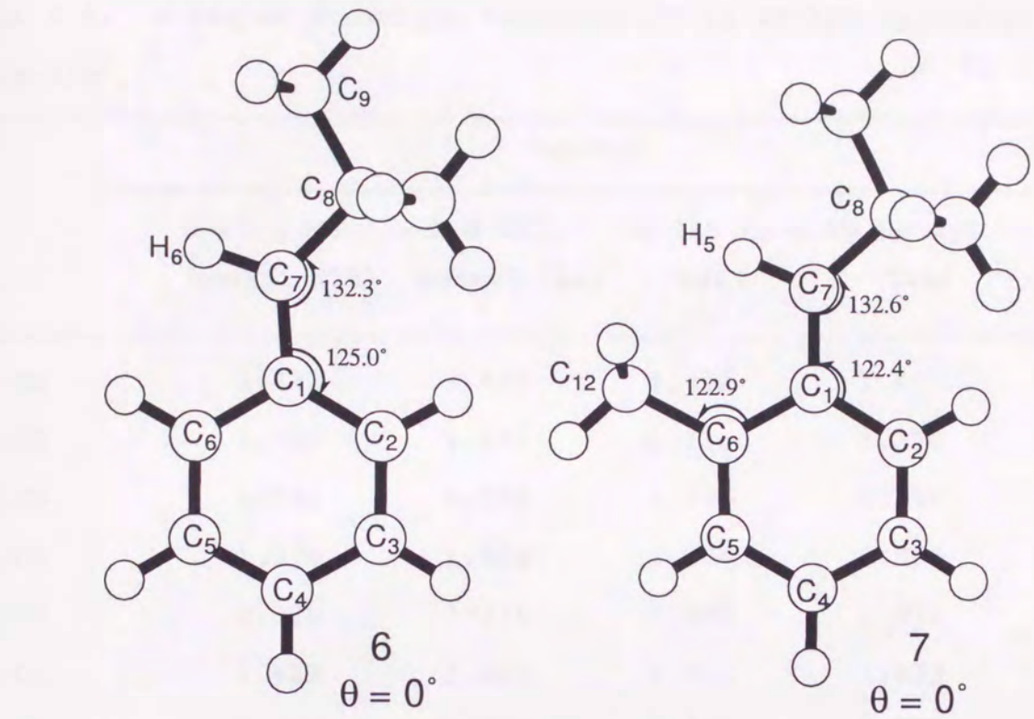

6
θ = 0°

7
θ = 0°

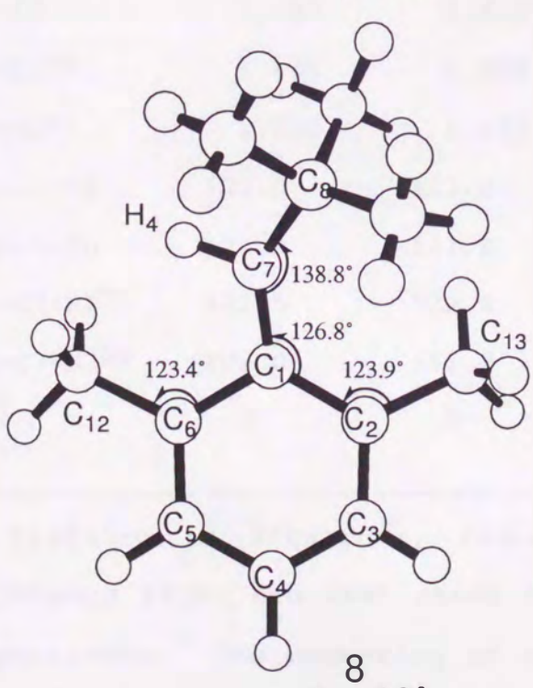

8
θ = 19°
∠$C_7C_1C_2C_3$ = 163.0°
∠$C_1C_2C_3C_4$ = 2.9°

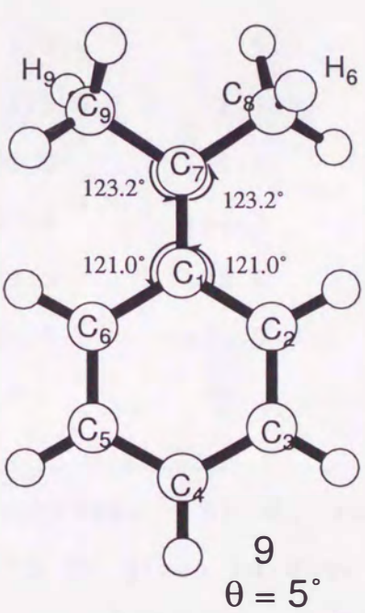

9
θ = 5°
∠$H_6C_8C_7C_1$ = -96.3°
∠$H_9C_9C_7C_1$ = -96.6°
∠$H_9C_9C_7$ = 107.5°
∠$H_6C_8C_7$ = 107.5°

Fig. 4-6. RHF/6-31G* optimized structures of **6**–**9**.

Table 4-4. Selected Geometric Parameters[a] of **10**-**12b** Optimized at RHF/6-31G*.

	Cations			
	α-Et-α-Me-benzyl (**10**)	α,α-Et_2-benzyl (**11**)	α-iso-Pr-α-Me-benzyl (**12a**)	(**12b**)
C1-C2	1.422	1.422	1.422	1.422
C2-C3	1.370	1.371	1.372	1.370
C3-C4	1.394	1.394	1.392	1.394
C4-C5	1.394	1.394	1.394	1.393
C5-C6	1.370	1.371	1.369	1.371
C6-C1	1.422	1.422	1.423	1.423
C1-C7	1.407	1.410	1.412	1.410
C7-R1[b]	1.496	1.500	1.506	1.519
C7-R2[b]	1.500	1.500	1.500	1.495
C7-C1-C2	121.0	121.0	122.0	121.9
C7-C1-C6	121.0	121.0	120.4	120.7
C1-C7-R1[b]	122.5	122.8	123.3	125.6
C1-C7-R2[b]	123.0	122.8	120.5	122.0
θ[c]	3	0	6	10

a) Distance in angstroms, angle in degrees. b) R_1 and R_2 correspond right and left atoms bonded to C_7 given in Fig. 4-7, respectively. The numbering of atom are given in Fig. 4-3. c) Mean dihedral angle of |180-∠R1C7C1C6| and |∠R2C7C1C6|.

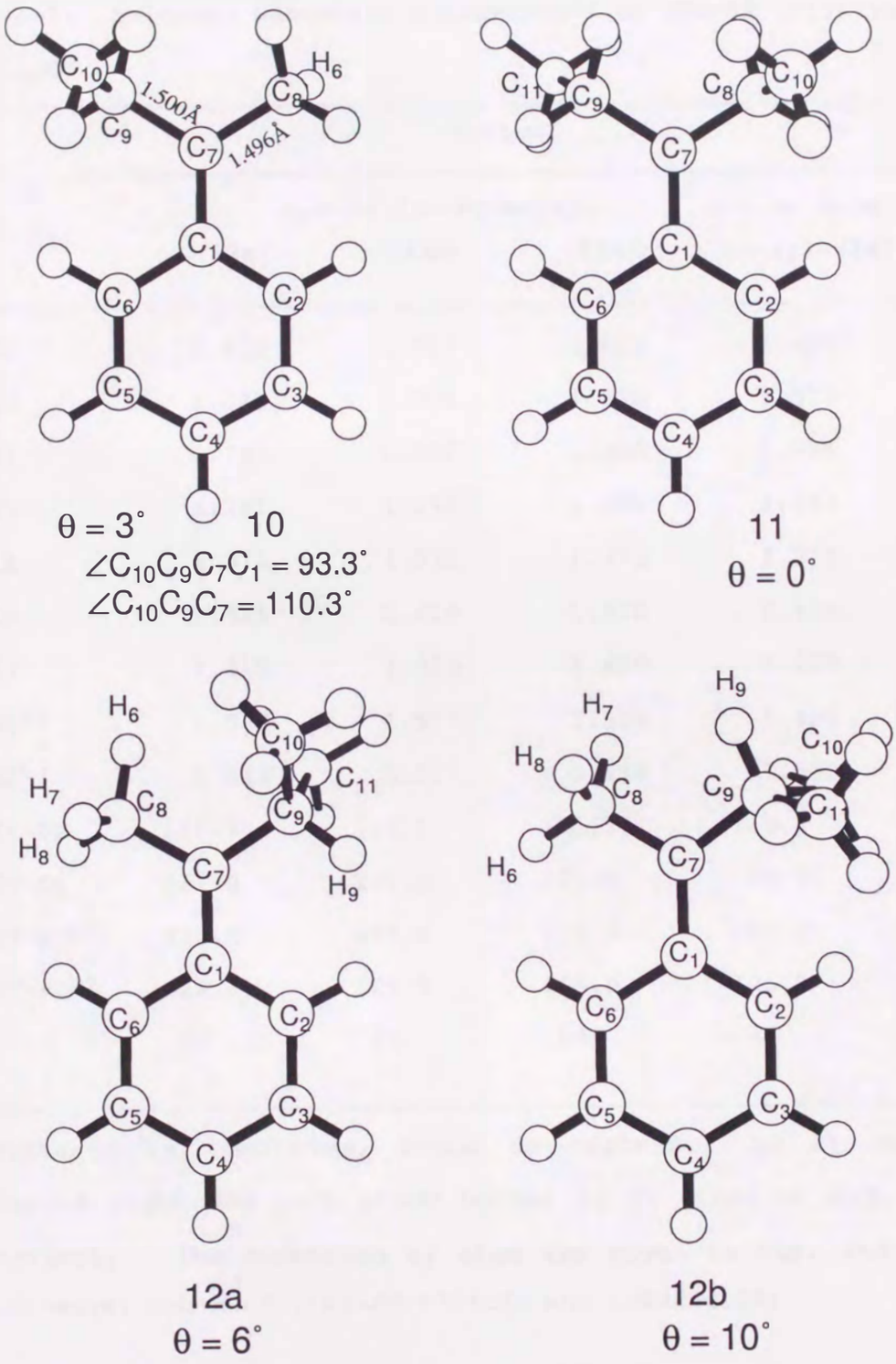

Fig. 4-7. RHF/6-31G* optimized structures of **10-12**.

Table 4-5. Selected Geometric Parameters[a] of **13a-14** Optimized at RHF/6-31G*.

	Cations			
	α,α-di-iso-Pr-benzyl			α-t-Bu-α-Me-
	(13a)	**(13b)**	**(13c)**	benzyl **(14)**
C1-C2	1.423	1.419	1.422	1.420
C2-C3	1.371	1.372	1.372	1.373
C3-C4	1.393	1.392	1.392	1.390
C4-C5	1.392	1.392	1.392	1.393
C5-C6	1.371	1.372	1.372	1.371
C6-C1	1.424	1.419	1.422	1.419
C1-C7	1.418	1.419	1.425	1.423
C7-R1[b]	1.522	1.517	1.518	1.497
C7-R2[b]	1.513	1.517	1.518	1.532
C7-C1-C2	121.6	121.3	121.5	119.3
C7-C1-C6	121.5	121.3	121.5	123.3
C1-C7-R1[b]	123.9	123.8	119.0	118.7
C1-C7-R2[b]	121.3	123.7	119.0	125.0
θ[c]	10	21	14	24

a) Distance in angstroms, angle in degrees. b) R_1 and R_2 correspond right and left atoms bonded to C_7 given in Fig. 4-8, respectively. The numbering of atom are given in Fig. 4-3. c) Mean dihedral angle of |180-∠R1C7C1C6| and |∠R2C7C1C6|.

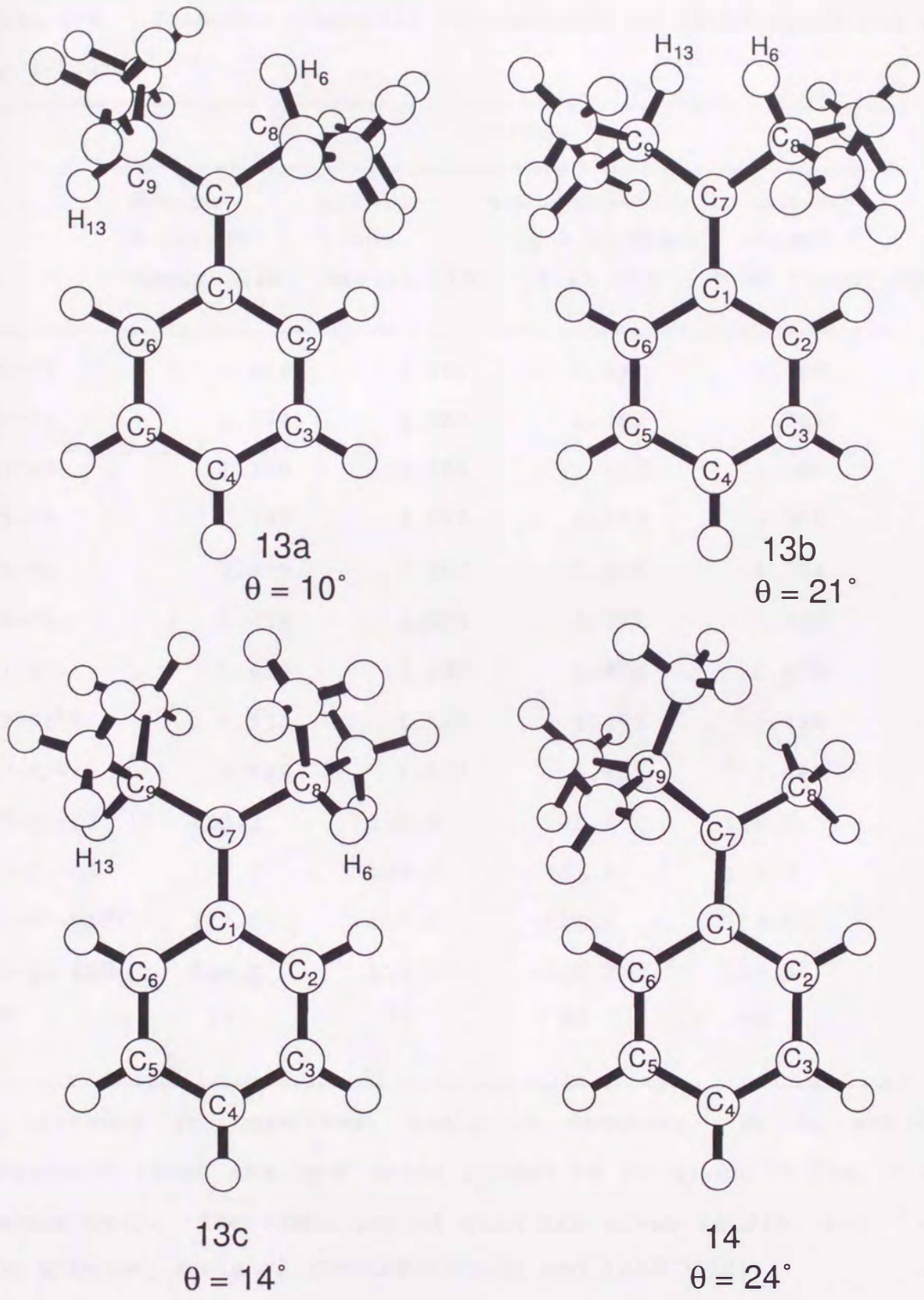

Fig. 4-8. RHF/6-31G* optimized structures of **13-14**.

Table 4-6. Selected Geometric Parameters[a] of **15**-**18** Optimized at RHF/6-31G*.

	Cations			
	α-t-Bu-α-iso-Pr-benzyl (**15**)	α,α-di-t-Bu-benzyl (**16**)	4-Me-benzobicyclo[2.2.2]octen-1-yl (**17**)	α,α-Me_2-benzyl (θ=90°fixed) (**18**)
C1-C2	1.414	1.394	1.402	1.390
C2-C3	1.374	1.383	1.380	1.384
C3-C4	1.390	1.386	1.392	1.386
C4-C5	1.389	1.386	1.384	1.386
C5-C6	1.375	1.383	1.390	1.384
C6-C1	1.414	1.394	1.377	1.390
C1-C7	1.434	1.482	1.470	1.478
C7-R1[b]	1.533	1.519	1.459	1.468
C7-R2[b]	1.522	1.519	1.459	1.468
C7-C1-C2	122.2	120.0	105.4	119.3
C7-C1-C6	120.2	120.0	131.4	119.3
C1-C7-R1[b]	122.8	117.0	116.2	119.6
C1-C7-R2[b]	120.2	117.0	116.2	119.6
θ[c]	34	76	90	90

a) Distance in angstroms, angle in degrees. b) R_1 and R_2 correspond right and left atoms bonded to C_7 given in Fig. 4-9, respectively. The numbering of atom are given in Fig. 4-3. c) Mean dihedral angle of |180-∠R1C7C1C6| and |∠R2C7C1C6|.

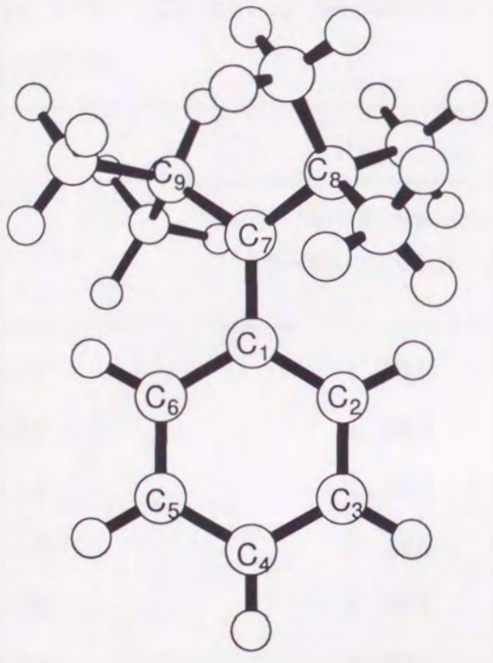

15
θ = 34°

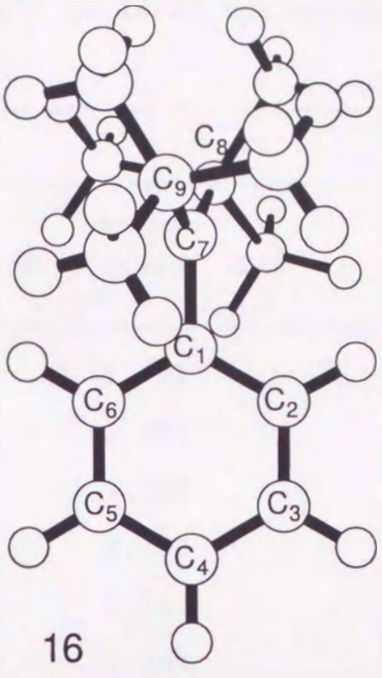

16
θ = 76°

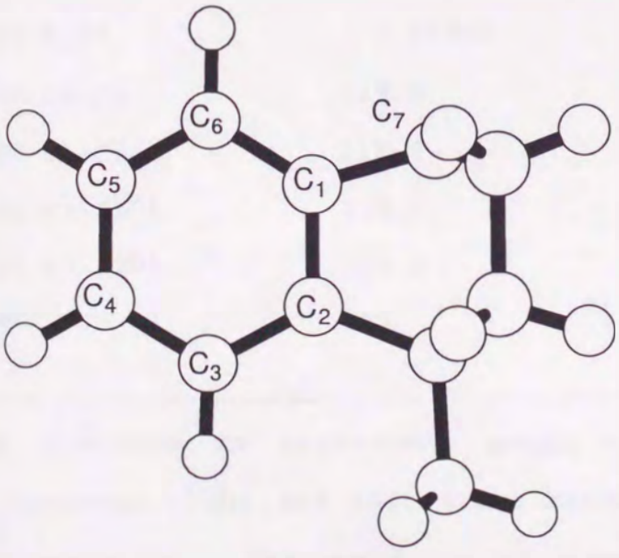

17
θ = 90°

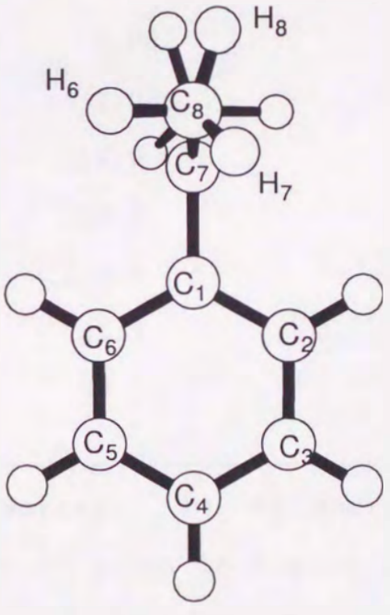

18
θ = 90°
∠$H_6C_8C_7C_1$ = 81.9°
∠$H_6C_8C_7$ = 103.0°

Fig. 4-9. RHF/6-31G* optimized structures of **15**–**18**.

Table 4-7. Selected Geometric Parameters[a] of **19**-**20** Optimized at RHF/6-31G*.

	Cations	
	α-CH_3-benzyl (θ=90°fixed) (**19**)	Benzyl (θ=90°fixed) (**20**)
C1-C2	1.391	1.393
C2-C3	1.384	1.383
C3-C4	1.386	1.386
C4-C5	1.386	1.386
C5-C6	1.384	1.383
C6-C1	1.392	1.393
C1-C7	1.466	1.454
C7-R1[b]	1.082[d]	1.082
C7-R2[b]	1.450[e]	1.082
C7-C1-C2	119.8	119.0
C7-C1-C6	118.5	119.0
C1-C7-R1[b]	118.6	121.9
C1-C7-R2[b]	124.0	121.9
θ[c]	90	90

a) Distance in angstroms, angle in degrees. b) R_1 and R_2 correspond right and left atoms bonded to C_7 given in Fig. 4-10, respectively. The numbering of atom are given in Fig. 4-3. c) Mean dihedral angle of |180-∠R1C7C1C6| and |∠R2C7C1C6|. d) Bond length between C_7 and H_6. e) Bond length between C_7 and C_8.

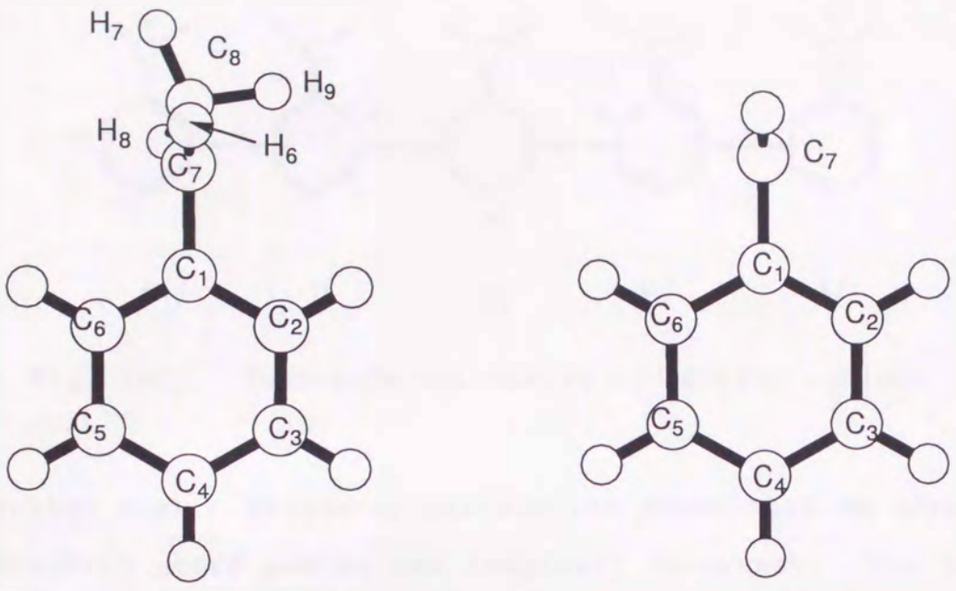

Fig. 4-10. RHF/6-31G* optimized structures of **19-20**.

structures shown in Fig. 4-11 elucidate partial alternation of single and double bonds in the benzene ring. This is a general prediction of resonance theory for charge delocalized benzylic cations, so that such tendency can commonly be seen for other species depending upon the contribution of the resonance stabilization.

α-Methylbenzyl Cation (4). α-Methylbenzyl cation was converged into two stationary conformations in C_1 symmetry: **4a** ($\angle H_9C_8C_7C_1=0^\circ$) and **4b** ($\angle H_9C_8C_7C_1=180^\circ$) as shown in Fig. 4-5. **4a** is more stable by 1.14 kcalmol^{-1} than **4b** at MP2/6-31G*//RHF/6-31G* +

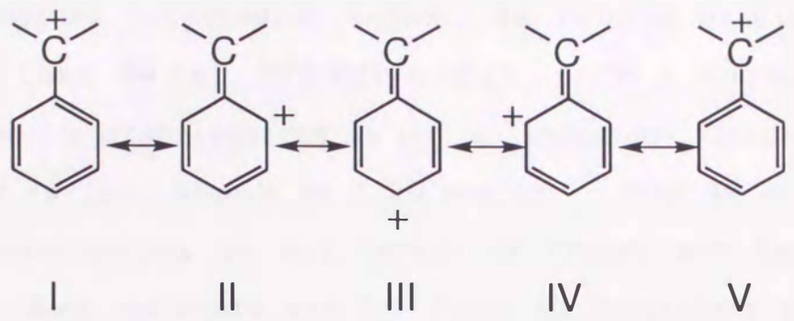

I II III IV V

Fig. 4-11. Resonance structures of bezylic cations.

ZPE (scaled 0.9). Frequency calculation shows that **4b** structure is transition state having one imaginary frequency. The normal mode associated with the imaginary frequency indicates that rotation of the methyl group leads to the lower energy structure. Then **4c** was optimized with 90° fixed dihedral angle ($\angle H_9C_8C_7C_1=90°$), and is less stable by 0.54 kcalmol^{-1} than **4a**. And when this constraint was removed, the geometry was converged to **4a**. Thus **4a** is considered to be the global minimum at the RHF/6-31G* level. **4a** should have a disadvantage compared to **4b** taking account of larger angle of $\angle H_9C_8C_7=114.8°$ for **4a** than $\angle H_9C_8C_7=111.0°$ for **4b** due to steric crowdness. Thus there is some stabilization factor which overwhelms such strain. The study of this point is in progress. Hartree-Fock theory may underestimate the hyperconjugation effect which exerts on the structure. For example, the bridged form for ethyl cation is global minimum at levels more than MP2, besides open cation is predominant at HF/6-31G* or HF/3-21G.[13] Thus the geometry optimization of **4a-c** was extended to MP2(FU)/6-31G* level. Although there may be a little stabilization by partial bridging for **4c** ($\angle H_9C_8C_7=107.4°$ which is

less than normal tetrahedral angle), **4a** is more stable by 0.56 $kcalmol^{-1}$ than **4c** at MP2(FU)/6-31G*. This suggests that hyperconjugative stabilization is not an important factor for this system. **4b** is less stable by 1.26 $kcalmol^{-1}$ than **4a** at the same level. Consequently, at all levels of theory and basis sets, hydrogen bridged structure was not found as stationary point, and **4a** is the most stable structure.

α-Trifluoromethylbenzyl Cation (1). Two minimum structures, **1a** ($\angle F_1C_8C_7C_1=180^\circ$) and **1b** ($\angle F_1C_8C_7C_1=0^\circ$), were found at RHF/6-31G* (Fig.4-4). The energy difference between these two conformations is very small; **1a** is 0.1 kcal/mol stable than **1b** contrary to α-methylbenzyl cation (**4**). A minimum structure with $\angle F_1C_8C_7C_1=90^\circ$ does not exist. Even at our final level (MP2/6-31G*//RHF/6-31G* + ZPE(scaled 0.9)), energy difference is also small; **1a** is more stable by 0.5 kcal/mol than **1b**. It is surprising that total energy of **1a** and **1b** is almost identical, since **1b** should have large disadvantage sterically more than **4a** and **4b** cases. Some stabilization factor must work on **1b** similar to the case for **4a**.

α-Trifluoromethyl-α-methylbenzyl Cation (2). Configurations of two α-substituents take a combinated one of those for CF_3 group in **1a** and CH_3 group in **4a** (Fig. 4-4). Other conformations have not been attempted.

2,2-Dimethyl-1-indanyl Cation (5). **5** is converged to almost C_S structure for all basis sets (Fig. 4-5). The five membered ring is in plane which is made by benzene framework. Although large steric strain exists in five membered ring included

in fused benzene ring ($\angle C_1C_7C_8$=113.0°, $\angle C_7C_8C_{11}$=103.2°, $\angle C_8C_{11}C_2$=104.4°, $\angle C_{11}C_2C_1$=110.0°, $\angle C_2C_1C_7$=109.4°), empty p orbital on C_7 should be parallel to benzene π system. Thus this system (**5**) is suitable for a secondary standard system which can conjugate fully with benzene π orbital.

α-*t*-Butylbenzyl Cation (6). Coplanarity between empty p orbital at benzylic position and benzene π system is held (θ=0°) for all basis sets, although large steric strain between *t*-Bu group and benzene ring results in $\angle C_7C_1C_2$=125.0° and $\angle C_1C_7R_1$=132.3° at RHF/6-31G* (Fig. 4-6). This supports the conclusion that resonance stabilization overwhelms steric hindrance to make transition state coplanar in this solvolysis system as described in chapter 2.

α-*t*-Butyl-*o*-methylbenzyl Cation (7). A energy minimum (Fig. 4-6) was found for **7** whose geometry is not basis set dependent. **7** corresponds o-methyl substituted **6**. However, the methyl group has no effective steric destabilization to change coplanarity (θ=0°). The *t*-Bu group is placed in the opposite side of o-Me group to avoid large steric interaction.

α-*t*-Butyl-*o*,*o*-dimethylbenzyl Cation (8). One more introduction of methyl group to **7** is expected to produce a large steric hindrance to change dihedral angle θ because the conformation such as **7** cannot be permitted any more. The structure for **8** optimized at RHF/6-31G* is shown in Fig. 4-6. Full resonance stabilization can not be accomplished (θ=19°) due to a large steric hindrance. Moreover this cation (**8**) minimizes the steric hindrance in a different manner compared to other tertiary congested system. The steric hindrance was diminished by not only

the rotation of *t*-Bu group around C_1-C_7 axis but also changes of several dihedral angles ($\angle C_7C_1C_2C_3$=163.0° and $\angle C_1C_2C_3C_4$=2.9°). This suggests that resonance effect intending the coplanar conformation has large contribution for stabilization of this cation. As argued in chapter 2, the r value in Yukawa-Tsuno treatment of 1.02 for solvolysis of precursor of **8** has been found in this laboratory, besides r=1.11 for that of **5** considering a secondary coplanar system. So that the decrease of resonance efficiency is only 10%. This may attributed to the large resonance stabilization effect for secondary systems compared to that for tertiary systems.

α,α-Dimethylbenzyl Cation (9). For **9**, geometriies are slightly basis set dependent; $\angle H_6C_8C_7C_1=\angle H_9C_9C_7C_1$=180° and θ=0° at RHF/STO-3G, while almost coplanar structures (θ=5°) at RHF/6-31G* (Fig. 4-6) and RHF/3-21G were given. Angles of $\angle C_9C_7C_1$, $\angle C_8C_7C_1$, $\angle C_6C_1C_7$, and $\angle C_2C_1C_7$ are larger by 2.1° than those for normal angle of sp_2 carbon on the average. It can be concluded that some steric strain exists even in this simplest tertiary benzylic cation in order to attain full resonance stabilization. At a glance, one may suggest the hyperconjugative stabilization for **9** according to the dihedral angles of $\angle H_6C_8C_7C_1$=-96.3° and $\angle H_9C_9C_7C_1$=-96.6°, and diminished angles of $\angle H_9C_9C_7=\angle H_6C_8C_7$=107.5°. But these configurations should be determined mainly by the steric requirement, because the hyperconjugation is not important even in **4**.

α-Ethyl-α-methylbenzyl Cation (10). One energy minimum structure **10** with $\angle C_{10}C_9C_7C_1$=93° (Fig. 4-7) was obtained at all

basis sets. That is, both initial geometries where dihedral angle $\angle C_{10}C_9C_7C_1$ are 0° and 180° were converged to **10** where the bond of C_9-C_{10} is parallel to the empty p orbital on C_7. One may suggest the important contribution of C-C hyperconjugation. However $\angle C_{10}C_9C_7$=110.3° which is larger than the angle of normal sp_3 tetrahedral carbon, and bond length of C_9-C_7 is 1.500Å which is longer than that for C_7-C_8 (1.496Å). Thus the configuration of ethyl group may not be attributed to effective hyperconjugation. Angles $\angle C_9C_7C_1$, $\angle C_8C_7C_1$, $\angle C_6C_1C_7$, and $\angle C_2C_1C_7$ in **10** are spread due to steric crowdness as similar as cation **9**.

α,α-Diethylbenzyl Cation (11). Geometry was converged to almost C_2 structure (Fig. 4-7) at all basis sets. Some steric strain exists like cations **9** and **10**.

α-Isopropyl-α-methylbenzyl Cation (12). Two minimum structures, **12a** and **12b** (Fig. 4-7), were obtained. Energy difference between these isomers and their geometries are not dependent on basis sets. Bulky isopropyl group takes configurations which make steric interaction with methyl group or phenyl group small by rotation of C_9-C_7 axis. H_6 of methyl group is inserted between C_{10} and C_{11} of isopropyl group (**12a**) or H_9 of isopropyl group put between H_7 and H_8 of methyl group (**12b**), making steric hindrance small. Dihedral angle θ of **12a** (θ=6°) is smaller than that of **12b** (θ=10°), so that loss of resonance interaction for **12a** should be smaller. The total energies of **12a** is 2.9 kcal/mol stabler than **12b**. This suggest that configuration of isopropyl group for **12b** has sterical disadvantage compared to that for **12a**.

α,α-Diisopropylbenzyl Cation (13). Three minimum structures were obtained by the combination of configuration of isopropyl groups for all basis sets (Fig. 4-8). At the final level (MP2/6-31G*//RHF/6-31G* + ZPE (scaled 0.9)), energy difference of these three species are small; **13a** (θ=10°) is more stable by 1.8 kcal/mol than **13b** and **13b** (θ=21°) is more stable by 0.8 kcal/mol than **13c**(θ=14°). The smallest dihedral angle θ (**13a**) is the most preferable conformation.

Highly Congested Cations: α-*t*-Butyl-α-methylbenzyl Cation (14), α-*t*-Butyl-α-isopropylbenzyl Cation (15), and α,α-di-*t*-Butylbenzyl Cation (16). In these cation systems, the bulkiness of one α-substituent was changed continuously from methyl (**14**) and isopropyl (**15**) to *tert*-butyl (**16**), besides another α-substituent was fixed to bulky *t*-Bu group (Figs. 4-8 and 4-9). These species can not maintain coplanarity between benzylic p orbital and benzene π system; there are very large steric hindrance which overwhelm resonance stabilization. As the bulkiness of α-substituents increase gradually, dihedral angles θ were increased continuously; θ=24° for **14**, θ=34° for **15**, and θ=76° for **16**. Geometries of **14** and **15** are not dependent on basis set. On the other hand, geometries of **16** are dependent on basis set; configuration of *t*-Bu group is changed to rotate around C_7-C_8 and C_7-C_9 axis about 5°, and dihedral angles θ was increased dramatically (22°) by the introduction of the split valence basis set keeping almost C_2 point group.

4-Methylbenzobicyclo[2.2.2]octen-1-yl Cation (17). At all basis sets geometry of **17** was converged to C_s structure (Fig.

4-9); empty p orbital on C_7 is set in perpendicular to benzene π system. Thus resonance stabilization does not exist supporting r=0 in solvolysis study of this laboratory.

90° Fixed Cations: α,α-Dimethylbenzyl Cation (θ=90° Fixed) (18), α-Methylbenzyl Cation (θ=90° Fixed) (19), and Benzyl Cation (θ=90° Fixed) (20). **18**, **19**, and **20** were optimized under the condition that the angle formed by the plane $R_1C_7R_2$ and the plane $C_1C_2C_6$ was fixed to 90° (Figs. 4-9 and 4-10). Carbon-carbon bond lengths of the phenyl rings are in the range 1.38 - 1.39Å which is almost the same for the carbon-carbon bond length of benzene (1.39Å at RHF/6-31G*). Thus these imaginary systems should take r value of 0 in Yukawa-Tsuno equation. The configurations of methyl groups for **18** and **19** are instructive. In **19**, C_8-H_9 bond is parallel with the vacant p orbital at C_7 ($\angle H_9C_8C_7C_1$=92°). Such configuration can not be found in coplanar cation **4**. Moreover angle of $\angle H_9C_8C_7$ is 100.4° which is smaller than that of normal tetrahedral angle. It is concluded that C-H hyperconjugation exists in this cation. Also stabilization by hyperconjugation should contribute to this localized cation **18**, contrary to the full conjugated cation **9**. That is, bond C_8-H_6 is almost parallel to benzene π system since $\angle H_6C_8C_7C_1$=81.9°, and $\angle H_6C_8C_7$ of 103.0° is smaller than the usual tetrahedral angle besides $\angle H_7C_8C_7$=113.7° and $\angle H_8C_8C_7$=112.2°. Charge at C_7 is delocalized into benzene π system in coplanar systems, so that requirement of hyperconjugative stabilization is little. However, for cations **18**, **19**, and **20**, charges at C_7 stay in no-aromatic

moiety similar to simple alkyl cation. This is the reason why hyperconjugation is effective in θ=90° fixed systems.

The energy difference between these 90° fixed cations (**18-20**) and the corresponding coplanar cations (**9**, **4a**, and **3**) can be approximated to the rotational barriers around C_1-C_7 axis. In practice, normal mode analysis in frequency calculation indicates that **18-20** are transition states concerning the rotation of C_1-C_7 axis. In addition, the perpendicular conformation is energetically maximum in all of the rotamers for benzyl cation,[12] while finite steric effect may exists for the coplanar structure of **9**, resulting in small dihedral angle (θ=5°). Since the rotational barrier has been used as a measure of the "resonance energy",[14] one can estimate the resonance energies for these species. Rotational barrier for each cation was summarized in Table 4-8. Basis sets and electron correlation do not affect the barriers seriously. At our final level (MP2/6-31G*//RHF/6-31G*) which does not include ZPE correlation, barriers (resonance energy) are 49.3 kcal/mol for benzyl cation, 33.8 kcal/mol for α-methylbenzyl cation, and 20.7 kcal/mol for α,α-dimethylbenzyl cation. Previously Houk et al. reported the rotational barrier of benzyl cation **3** (45.4 kcal/mol) at HF/3-21G level which agrees with the present result. One methyl substitution to the benzylic position lowers the rotational barrier by 15 kcal/mol. This may be attributed to the resonance stabilization of each benzylic cation. The primary benzyl cation **3** is required larger magnitude of conjugation in order to stabilize the total energy. On the other

Table 4-8. Rotational Barrier[a] (kcal mol^{-1}) of Benzylic Cation.

Cations	RHF/ STO-3G	RHF/ 3-21G	RHF/ 6-31G*	MP2/6-31G*// RHF/6-31G*[b]
benzyl cation				
	47.086	45.390	45.887	49.302
α-methylbenzyl cation				
	34.548	31.840	32.440	33.771
α,α-dimethylbenzyl cation				
	22.011	19.045	19.685	20.740

a) Rotational barriers were estimated by the total energy difference between coplanar and orthogonal (90° fixed) structures; E(**18**)-E(**9**) for α,α-dimethylbenzyl cation, E(**19**)-E(**4a**) for α-methylbenzyl cation, and E(**20**)-E(**3**) for benzyl cation. b) ZPE are not included.

hand, tertiary α,α-dimethylbenzyl cation (**9**) is stabilized by the electronic effect of α-methyl group, so that the requirement of resonance stabilization is small. It is worthy to note that the r value in Yukawa-Tsuno equation runs parallel with rotational barriers of corresponding benzylic cations. This is instructive, because the r value can be connected to the resonance energy for these structurally similar species.

Inspection of Ab Initio Energy. As discussed in chapter 3, we determined the intrinsic stabilities of benzylic cations in gas phase according to the isodesmic reactions (4-2) or (4-3).

$$Ph(R_1)C{=}R_2 + Ph(CH_3)C(+)CH_3 = Ph(R_1)C(+)R_2 + Ph(CH_3)C{=}CH_2.$$

(4-2)

$$Ph(R_1)C(R_2)Cl + Ph(Me)C(+)Me = Ph(R_1)C(+)R_2 + Ph(Me)C(Me)Cl.$$

(4-3)

Intrinsic gas phase stabilities of **1**, **2**, **3**, **4**, **9**, **10**, **11**, **12**, **13**, and **14** have been determined on the basis of proton transfer equilibria (Eq. (4-2)) or chloride transfer equilibria (Eq. (4-3)) using ICR technique. Thus an inspection of ab initio energy can be made. Total energies of benzylic cations are shown in Table 4-9. Energies of corresponding olefins and chlorides are summarized in Table 4-10. At all levels of theories and basis sets, calculated intrinsic stabilities of benzylic cations are compared to experimental values.

At RHF/STO-3G, E(calcd) = 1.22 E(exptl) + 0.23. (4-4)

(R=0.978, SD=±2.1, and n=10)

At RHF/3-21G, E(calcd) = 1.46 E(exptl) - 0.76. (4-5)

(R=0.977, SD=±2.6, and n=10)

At RHF/6-31G*, E(calcd) = 1.34 E(exptl) - 0.26. (4-6)

(R=0.991, SD=±1.5, and n=10)

At MP2/6-31G*//RHF/6-31G* + ZPE,

E(calcd) = 1.20 E(exptl) - 0.97. (4-7)

(R=0.989, SD=±1.5, and n=10)

The 6-31G* basis sets seems to reproduce the experimental results well regardless theoretical levels. In Fig. 4-12, calculated free energy changes at the final level are plotted against experimental values. Although the slope is not unity, the correlation is satisfactory (±1.5 kcal/mol) for these benzylic cations.

Table 4-9. Total Energies (-au) of Substituted Benzyl Cations.

species[a]	theoretical level				
	RHF/ STO-3G	RHF/ 3-21G	RHF/ 6-31G*	MP2/6-31G*// RHF/6-31G*	ZPE[b]
1a	596.606702	601.162418	604.485146	605.972559	-0.131997(0)
1b	596.605947	601.162416	604.484959	605.971916	-0.132222(0)
2	635.202371	639.997766	643.531254	645.156203	-0.161853(0)
3	265.654106	267.380453	268.886732	269.740682	-0.125692(0)
4a	304.252772	306.215505	307.937589	308.925073	-0.155503(0)
4b	304.251557	306.214174	307.935767	308.923118	-0.155213(1)
4c	304.252162	306.214852	307.936726	308.924201	-0.155346(0)[c]
5	418.862147	421.531556	423.892862	425.275269	-0.223752(0)
6	419.990743	422.675104	425.037309	426.426977	-0.246438(0)
7	458.577432	461.497707	464.075480	465.599353	-0.276214(0)
8	497.145738	500.303690	503.097692	504.760333	-0.306524(0)
9	342.844810	345.044469	346.981039	348.103622	-0.185231(0)
10	381.427386	383.866601	386.016827	387.271753	-0.216495(0)
11	420.009129	422.688605	425.052517	426.440163	-0.247754(0)
12a	420.006295	422.686123	425.049712	426.439329	-0.246707(0)
12b	420.000969	422.679914	425.044513	426.434732	-0.246712(0)
13a	497.159483	500.319048	503.110505	504.769321	-0.308218(0)
13b	497.155158	500.314478	503.106549	504.766081	-0.307844(0)
13c	497.156050	500.314792	503.106689	504.765623	-0.308815(0)
14	458.572677	461.494615	464.069696	465.599223	-0.276848(0)
15	535.723141	539.125355	542.127343	543.927161	-0.337824(0)
16	574.284700	577.932656	581.142841	583.082042	-0.367368(0)
17	494.823414	497.974423	500.751395	502.404530	-0.263034(0)
18	342.809734	345.014119	346.949669	348.070571	-0.182525(1)
19	304.197717	306.164765	307.885892	308.871256	-0.152307(1)
20	265.579070	267.308120	268.813607	269.662114	-0.122504(1)

a) Number of compound refered to Figs. 4-1 and 4-2. b) Zero-point energies (uncorrected) at the RHF/6-31G* level. Values in parentheses are the number of imaginary frequencies in frequency calculation. c) Not minimum.

Table 4-10. Total Energies (-au) of 1- or 2-Substituted Styrenes and Substituted Benzyl Chlorides.

species	theoretical level				
	RHF/ STO-3G	RHF/ 3-21G	RHF/ 6-31G*	MP2/6-31G*// RHF/6-31G*	ZPE[a]
R1,R2,R3[b] (Styrenes)					
CF3,H,H	634.800157	639.688076	643.205570	644.845463	-0.149732(0)
H,H,H	303.834446	305.872493	307.585474	308.591299	-0.143094(0)
Me,H,H	342.416428	344.692880	346.621454	347.762116	-0.173203(0)
Et,H,H	380.995755	383.512388	385.655448	386.928574	-0.203895(0)
Me,Me,H(Z)	380.999100	383.513822	385.657371	386.930950	-0.202987(0)
Me,Me,H(E)	380.998918	383.512310	385.656615	386.930293	-0.203083(0)
Et,Me,H(Z)	419.578771	422.332935	424.691400	426.097947	-0.233756(0)
Et,Me,H(E)	419.577853	422.331798	424.690513	426.096790	-0.233903(0)
i-Pr,Me,Me(a)	496.735797	499.968061	502.754379	504.432724	-0.293632(0)
i-Pr,Me,Me(b)	496.731493		502.750241	504.427980	-0.293727(0)
Me,Me,Me	419.579022	422.331958	424.690005	426.098988	-0.232568(0)
i-Pr,H,H(a)	419.572903	422.331302	424.687824	426.095753	-0.234155(0)
i-Pr,H,H(b)	419.572103	422.330551	424.686687	426.094893	-0.233831(0)
t-Bu,Me,Me	535.303463	538.777763	541.775340	543.593682	-0.323904(0)
t-Bu,H,H	458.147869	461.149001	463.716832	465.263000	-0.264107(0)
R1,R2[c] (Benzyl Chlorides)					
CF3,H	1051.435026	1058.765992	1064.255804	1065.906737	-0.134728(0)
H,H	720.475497	724.958133	728.640040	729.654920	-0.128619(0)
Me,Me	797.635122	802.603080	806.708007	807.995996	-0.188630(0)
t-Bu,t-Bu	1029.066551	1035.479692	1040.857001	1042.968557	-0.371391(0)

a) Zero-point energies (uncorrected) at the RHF/6-31G* level. Values in parentheses are the number of imaginary frequencies in frequency calculation. b) R1 are substituents which connect to α-carbon. R2 and R3 are substituents which connect to β-carbon. c) R1 and R2 are substituents which connect to benzylic carbon.

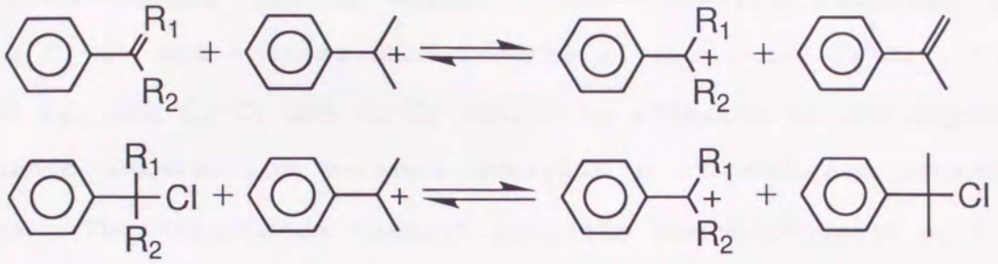

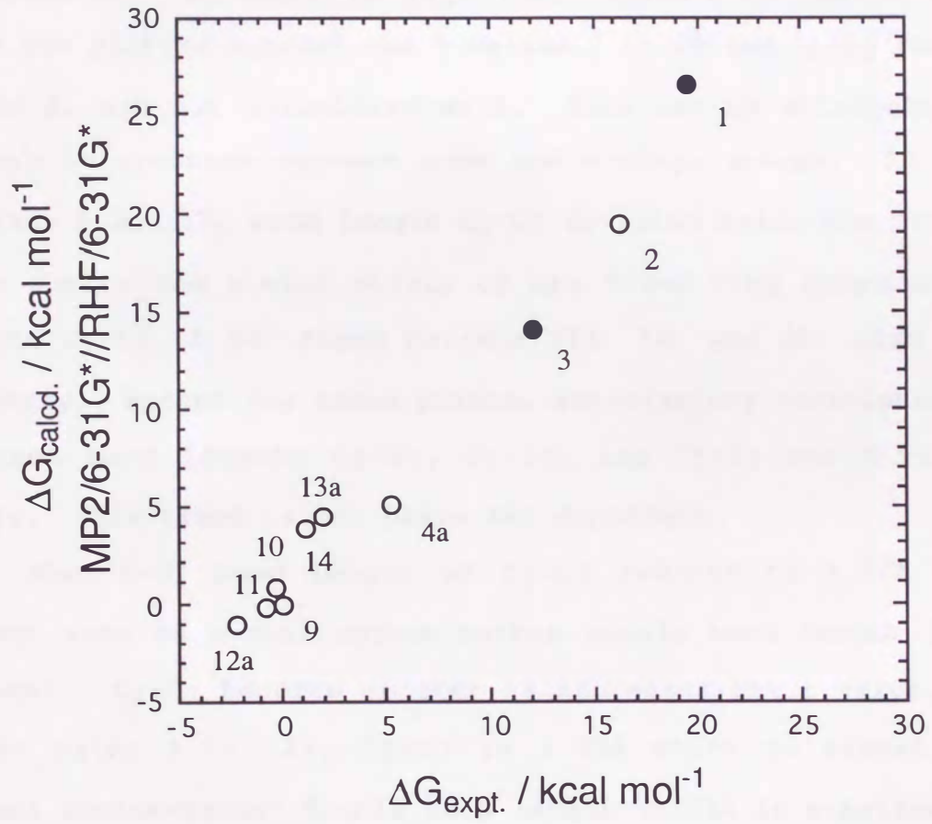

Fig. 4-12. Comparison of free energy change between calculated (MP2/6-31G*//RHF/6-31G* + ZPE(scaled 0.9)) and experimental value, determined by proton transfer (open circle) or chloride transfer (closed circle) equilibria. Number correspond those for species in Figs. 4-1 and 4-2.

Bond Length vs. r Value. For benzylic cations, bond length C_1-C_7 and average bond lengths of C_1-C_2 and C_6-C_1 , C_2-C_3 and C_5-C_6, and C_3-C_4 and C_4-C_5 should be affected by the degree of resonance interaction between benzylic p orbital and benzene π system. The "resonance theory" predicts the elongation of C_1-C_2 and C_3-C_4, and shortening of C_1-C_7 and C_2-C_3 as increase of conjugation. As shown in Fig. 4-13, these bond length at RHF/6-31G* are plotted against the r values. C_1-C_7 and C_1-C_2 for cations **7** and **8**, are not correlated well. This may be attributed to the steric interaction between *o*-Me and α-alkyl groups. In cases of cations **5** and **17**, bond length C_1-C_7 deviates below the correlation line due to the steric strain of the fused ring structure. Bond length C_1-C_7 of 90° fixed cations (**18**, **19**, and **20**) also deviated slightly. Except for these points, satisfactory correlation exists between bond lengths C_1-C_7, C_1-C_2, and C_2-C_3 and r value as a whole. This trend is not basis set dependent.

When r=0, bond length of C_1-C_7 reaches to 1.52Å which is almost same as normal carbon-carbon single bond length (1.54Å in ethane). C_1-C_7 becomes shorter as increases the r value. When r value takes 1.51 (**1**), C_1-C_7 is 1.35Å which is almost same as normal carbon-carbon double bond length (1.33Å in ethylene). Bond length C_1-C_7 changes drastically with the resonance demand. When r=0, bond lengths C_1-C_2, C_2-C_3, and C_3-C_4 are 1.39Å which are the same as carbon-carbon bond length of benzene. As the r value increases, C_1-C_2 and C_3-C_4 increases but C_2-C_3 decreases. The slope of C_1-C_2 is twice as large as that of C_3-C_4. This tendency

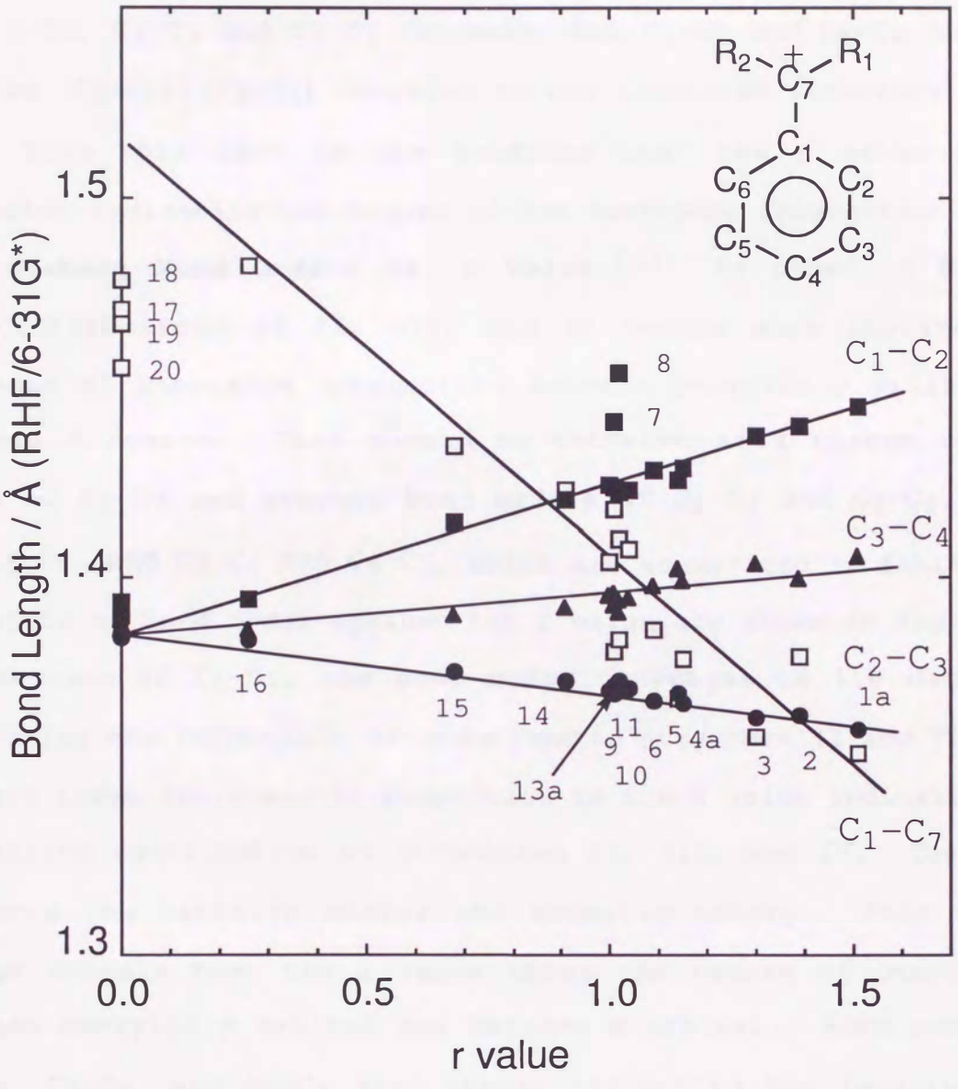

Fig. 4-13. Bond length vs r values in Yukawa-Tsuno equation for benzylic cations. Numbers correspond those for species in Figs. 4-1 and 4-2.

agrees well with the prediction of the resonance theory. Assuming the equivalent contributions of five resonance structures shown in Fig. 4-11, C_1-C_7 and C_2-C_3 decrease, but C_1-C_2 and C_3-C_4 increase keeping $(C_1\text{-}C_2)>(C_3\text{-}C_4)$ compared to the localized structure (I and V). Thus this plot is the evidence that the r value is the parameter indicating the degree of the resonance interaction.

Wieberg Bond Orders vs. r Value.[15] As shown in Fig. 4-11, contributions of II, III, and IV become more important as increase of resonance interaction between benzylic p orbital and benzene π system. This should be detected as a change of bond order of C_1-C_7 and average bond orders of C_1-C_2 and C_6-C_1, C_2-C_3 and C_5-C_6, and C_3-C_4 and C_4-C_5, which are summarized in Table 4-11. The plots of bond order against the r value are shown in Fig. 4-14. In the case of C_1-C_7, the bond order converges to 1.0 when r=0, reflecting the importance of unconjugated structure (I and V). The Wieberg index increases in proportion to the r value indicating the increasing contribution of structures II, III, and IV. The C_1-C_7 connects the cationic center and aromatic moiety. This way of change reveals that the r value shows the degree of overlapping between benzylic p orbital and benzene π orbital. Bond orders of C_1-C_2, C_2-C_3, and C_3-C_4 also change reflecting the importance of contribution of each cannonical structure (I-V) in Fig. 4-11. When r=0, these Wieberg indices take 1.4, which is an intermediate value between single and double bond. As the r increases, C_2-C_3 increases but C_1-C_2 and C_3-C_4 decrease. All these behaviors are consistent to the prediction of resonance theory. Consequently

Table 4-11. Wieberg Bond Orders from NBO Analysis Calculated at RHF/6-31G* for Benzylic Cations.

species[a]	Wieberg bond order[b]			
	C_1-C_7[c]	C_1-C_2[d]	C_2-C_3[e]	C_3-C_4[f]
1a	1.6224	1.1336	1.5847	1.3293
2	1.5058	1.1659	1.5608	1.3472
3	1.5835	1.1584	1.5671	1.3432
4a	1.4648	1.1931	1.5432	1.3611
5	1.4831	1.1778	1.5209	1.3688
6	1.4472	1.2026	1.5359	1.3662
7	1.4855	1.1763	1.5267	1.3621
8	1.4918	1.1630	1.507	1.3659
9	1.3632	1.2254	1.5244	1.3747
10	1.3519	1.2311	1.5208	1.3772
11	1.3433	1.2353	1.5179	1.3792
13a	1.3377	1.2390	1.5152	1.3808
14	1.3057	1.2531	1.5074	1.3859
15	1.2493	1.2789	1.4921	1.3963
16	1.0485	1.3700	1.4441	1.4278
17	1.0173	1.3710	1.4224	1.4331
18	1.0169	1.3857	1.4354	1.4333
19	1.0386	1.3808	1.4364	1.4324
20	1.0625	1.3722	1.4378	1.4311

a) Numbers correspond those in Figs. 4-1 and 4-2. b) Ref. 16. c) Wieberg bond orders of bond C_1-C_7. d) Average Wieberg bond orders of bond C_1-C_2 and C_6-C_1. e) Average Wieberg bond orders of bond C_2-C_3 and C_5-C_6. f) Average Wieberg bond orders of bond C_3-C_4 and C_4-C_5.

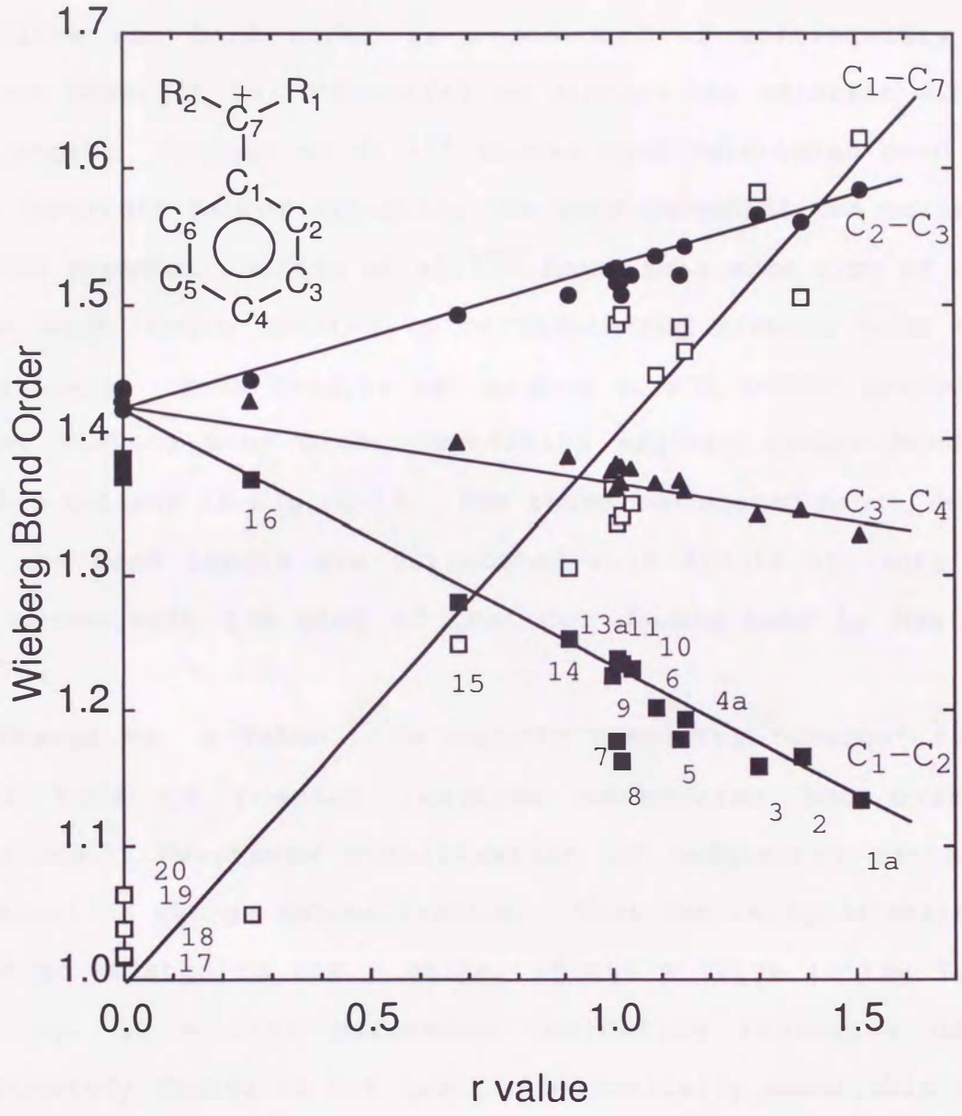

Fig. 4-14. Wieberg bond orders from NBO analtsis (RHF/6-31G*) vs r values in Yukawa-Tsuno equation for benzylic cations. Numbers correspond those for species in Figs. 4-1 and 4-2.

this indicates the increasing interaction between C_7 and aromatic moiety as the r value increases.

Since the bond order is a standard of multiplicity of a covalent bond, it is interesting to discuss the relation with the bond length. Coulson et al.[16] showed that calculated bond order is an important factor affecting the bond length in conjugated and aromatic systems. Martin et al.[17] found that some type of carbon carbon bond length relates to corresponding Wieberg bond orders respectively. Bond lengths calculated at RHF/6-31G* are plotted against Wieberg bond order concerning sp_2-sp_2 carbon bonds for benzylic cations in Fig. 4-15. For these conjugated bonds, Wieberg index and bond length are correlated with single straight line. This agrees with the plot of that for double bond by Martin et al..[17]

Charge vs. r Value. In organic chemistry "charge" is very useful tool to predict reaction mechanisms and molecular properties. Resonance stabilization of conjugated cations is equivalent to charge delocalization. Thus the charge distribution should be related to the r value, if the r value in the Yukawa-Tsuno Eq. is a real parameter indicating resonance degree. Unfortunately charge is not quantum mechanically observable though it is easy to understand intuitively. Several arbitrary methods have been proposed to estimate atomic charges.[18] The Mulliken population analysis (MPA)[10] and natural population analysis (NPA)[9] are selected in order to discuss the relation between charges and the r value. Atomic charges on each position of phenyl

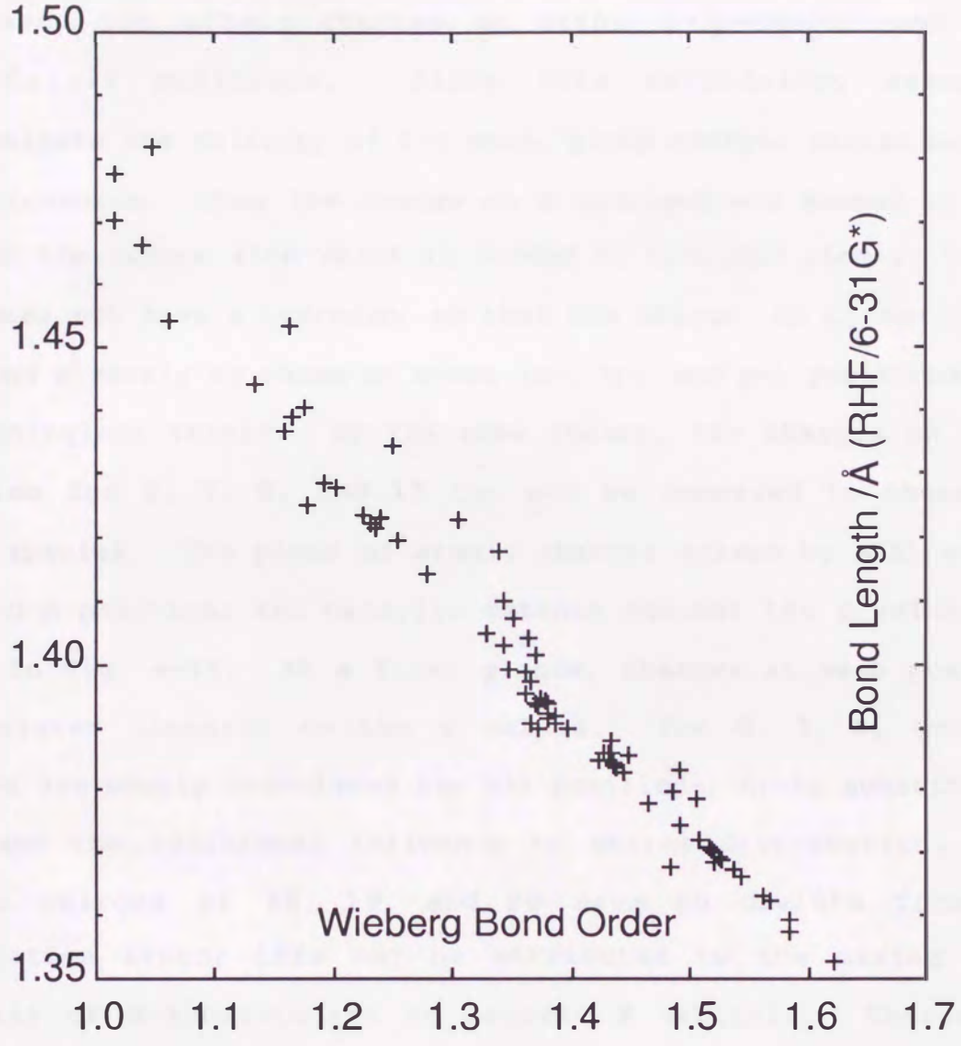

Fig. 4-15. Bond length (RHF/6-31G*) vs Wieberg bond orders of conjugated bonds for benzylic cations.

ring for benzylic cations which are calculated by MPA and NPA were summarized in Tables 4-12 and 4-13, respectively. Average values were used for atomic charges on ortho ($(C_2+C_6)/2$) and meta ($(C_3+C_5)/2$) positions. Since this methodology seems to overestimate the polarity of C-H bond, group charges should be used for discussion. Thus the charge on a hydrogen was summed up into that on the carbon atom which is bonded to hydrogen atoms. The C_1 atom does not have a hydrogen, so that the charge on C_1 can not be compared directly to those on other (o-, m-, and p-) positions, and is meaningless itself. By the same reason, the charges on ortho position for **5**, **7**, **8**, and **17** can not be compared to those for other species. The plots of atomic charges (given by MPA) on o-, m-, and p-positions for benzylic cations against the r values are shown in Fig. 4-16. At a first glance, charges at each position are related linearly to the r values. For **5**, **7**, **8**, and **17**, charges are poorly correlated for all positions; ortho substitution may have the additional influence to charge distribution. The atomic charges of **18**, **19**, and **20** seem to deviate from the correlation lines; this may be attributed to the mixing of σ orbitals of α-substituents to benzene π orbitals. Charges of species at each position excluding **5**, **7**, **8**, **17**, **18**, **19**, and **20** are correlated with r values as shown below. For charges on ortho position (P(ortho)) given by MPA,

$$P(ortho) = 0.125\ r + 0.016 \qquad (4\text{-}8)$$

$$(R=0.987\ SD=\pm 0.0070).$$

Table 4-12. Atomic Charges Given by Mulliken Population Analysis for Benzylic Cations (RHF/6-31G*).

species[a]	charge[b] (RHF/6-31G*)			
	C_1	ortho[c]	meta[d]	para[e]
1a	-0.030	0.211	0.053	0.233
2	-0.074	0.191	0.046	0.211
3	-0.024	0.189	0.051	0.213
4a	-0.050	0.164	0.046	0.190
5	-0.062	(0.142)[f]	0.030	0.173
6	-0.040	0.154	0.041	0.182
7	-0.062	(0.145)[f]	0.012	0.192
8	-0.100	(0.129)[f]	-0.009	0.192
9	-0.068	0.140	0.043	0.171
10	-0.066	0.137	0.041	0.166
11	-0.066	0.135	0.039	0.163
13a	-0.076	0.133	0.034	0.160
14	-0.074	0.123	0.039	0.153
15	-0.078	0.110	0.036	0.137
16	-0.088	0.054	0.053	0.077
17	-0.053	(0.074)[f]	0.037	0.073
18	-0.081	0.043	0.069	0.078
19	-0.107	0.055	0.073	0.085
20	-0.134	0.071	0.080	0.095

a) Numbers correspond those in Figs. 4-1 and 4-2. b) Atomic charges on each position with hydrogens summed into heavy atoms given by MPA (Mulliken Population Analysis). c) Average atomic charge of C_2 and C_6. d) Average atomic charge of C_3 and C_5. e) Atomic charge of C_4. f) Invalid data (See text).

Table 4-13. Atomic Charges Given by Natural Population Analysis for Benzylic Cations (RHF/6-31G*).

species[a]	charge[b] (RHF/6-31G*)			
	C_1	ortho[c]	meta[d]	para[e]
1a	-0.213	0.263	-0.032	0.339
2	-0.233	0.243	-0.027	0.300
3	-0.251	0.249	-0.031	0.310
4a	-0.254	0.223	0.022	0.269
5	-0.238	(0.198)[f]	0.029	0.263
6	-0.253	0.218	0.025	0.259
7	-0.250	(0.201)[f]	-0.043	0.276
8	-0.237	(0.260)[f]	-0.058	0.274
9	-0.256	0.200	-0.016	0.239
10	-0.257	0.195	0.015	0.232
11	-0.255	0.189	-0.013	0.224
13a	-0.255	0.190	0.018	0.223
14	-0.249	0.174	-0.009	0.209
15	-0.244	0.148	0.000	0.180
16	-0.198	0.051	0.047	0.080
17	-0.183	(0.023)[f]	0.053	0.073
18	-0.210	0.035	0.066	0.071
19	-0.238	0.043	0.069	0.078
20	-0.281	0.052	0.073	0.088

a) Numbers correspond those in Figs. 4-1 and 4-2. b) Atomic charges on each position with hydrogens summed into heavy atoms given by NPA (Natural Population Analysis). c) Average atomic charge of C_2 and C_6. d) Average atomic charge of C_3 and C_5. e) Atomic charge of C_4. f) Invalid data (See text).

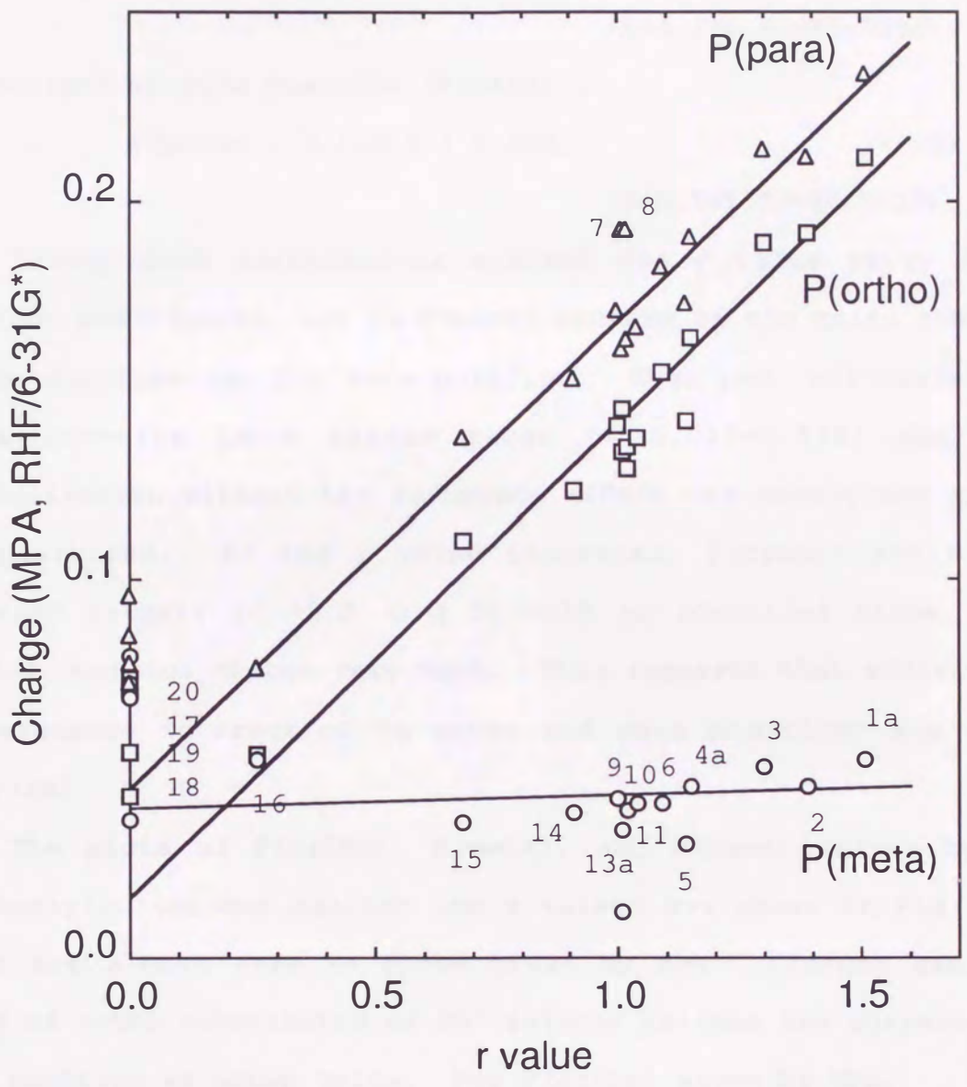

Fig. 4-16. Mulliken population (summed into heavy atom) on ortho (P(ortho)), meta (P(meta)), and para (P(para)) position of phenyl ring (RHF/6-31G*) vs r values in Yukawa-Tsuno equation for benzylic cations. Numbers correspond to those for species in Figs. 4-1 and 4-2.

For charges on meta position (P(meta)),

$$P(meta) = 0.003\ r + 0.040 \qquad (4\text{-}9)$$

(R=0.176 SD=±0.0066).

For charges on para position (P(para)),

$$P(para) = 0.123\ r + 0.045 \qquad (4\text{-}10)$$

(R=0.991 SD=±0.0057).

Fairly good correlations against the r value exist in the P(ortho) and P(para), but in P(meta) because of the small change of charge distribution for meta position. When r=0, all correlation lines converge in a narrow range of 0.015-0.045; degree of delocalization without the resonance effect are nearly the same in all positions. As the r value increases, P(ortho) and P(para) increase largely to +0.2 (r=1.5) with an identical slope, while P(meta) does not change very much. This suggests that efficiencies of resonance interaction on ortho and para positions are almost identical.

The plots of P(ortho), P(meta), and P(para) (given by NPA) for benzylic cations against the r values are shown in Fig. 4-17, which are almost same as those given by MPA. Charges excluding those of ortho substituted or 90° twisted cations are correlated in each position as shown below. For P(ortho) given by NPA,

$$P(ortho) = 0.168\ r + 0.023 \qquad (4\text{-}11)$$

(R=0.984 SD=±0.0104).

For P(meta),

$$P(meta) = -0.055\ r + 0.056 \qquad (4\text{-}12)$$

(R=0.706 SD=±0.0188).

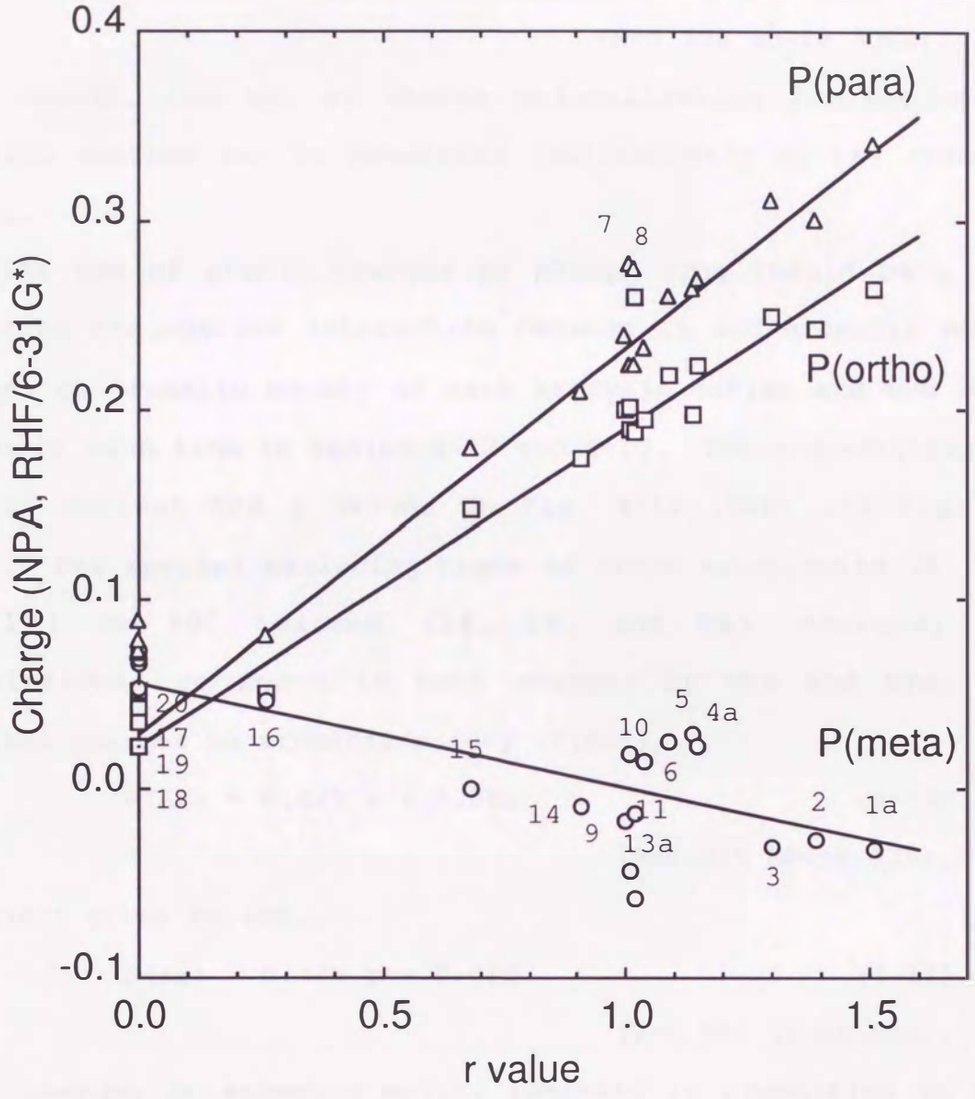

Fig. 4-17. Natural population (summed into heavy atom) on ortho (P(ortho)), meta (P(meta)), and para (P(para)) position of phenyl ring (RHF/6-31G*) vs r values in Yukawa-Tsuno equation for benzylic cations. Numbers correspond to those for species in Figs. 4-1 and 4-2.

For P(para),

$$P(para) = 0.204\ r + 0.029 \qquad (4\text{-}13)$$

(R=0.990 SD=±0.0098).

As a result, the way of charge delocalization for conjugative benzylic cations can be predicted qualitatively by the resonance theory.

The sum of atomic charges on phenyl ring should be a probe measuring conjugative interaction between C_7 and aromatic moiety. Charges on aromatic moiety of each benzylic cation are sum of the values of each line in Tables 4-12 and 4-13. These quantities were plotted against the r values in Fig. 4-18 (MPA) and Fig. 4-19 (NPA). For species excluding those of ortho substituted (**5**, **7**, **8**, and **17**) or 90° twisted (**18**, **19**, and **20**) cations, good correlations are found in both charges by MPA and NPA. For Mulliken charges on aromatic moiety (P(Ar)),

$$P(Ar) = 0.425\ r + 0.051 \qquad (4\text{-}14)$$

(R=0.966 SD=±0.039).

For P(Ar) given by NPA,

$$P(Ar) = 0.403\ r - 0.055 \qquad (4\text{-}14)$$

(R=0.985 SD=±0.025).

Total charges on aromatic moiety increase in proportion to the r values. This suggests that delocalization to the phenyl ring is the controlling factor of the r value.

Comparison of theoretically obtained θ_{calc} and experimentally estimated θ_{exptl}. As argued in the section of "Wieberg bond orders vs. r value," the r value should also be

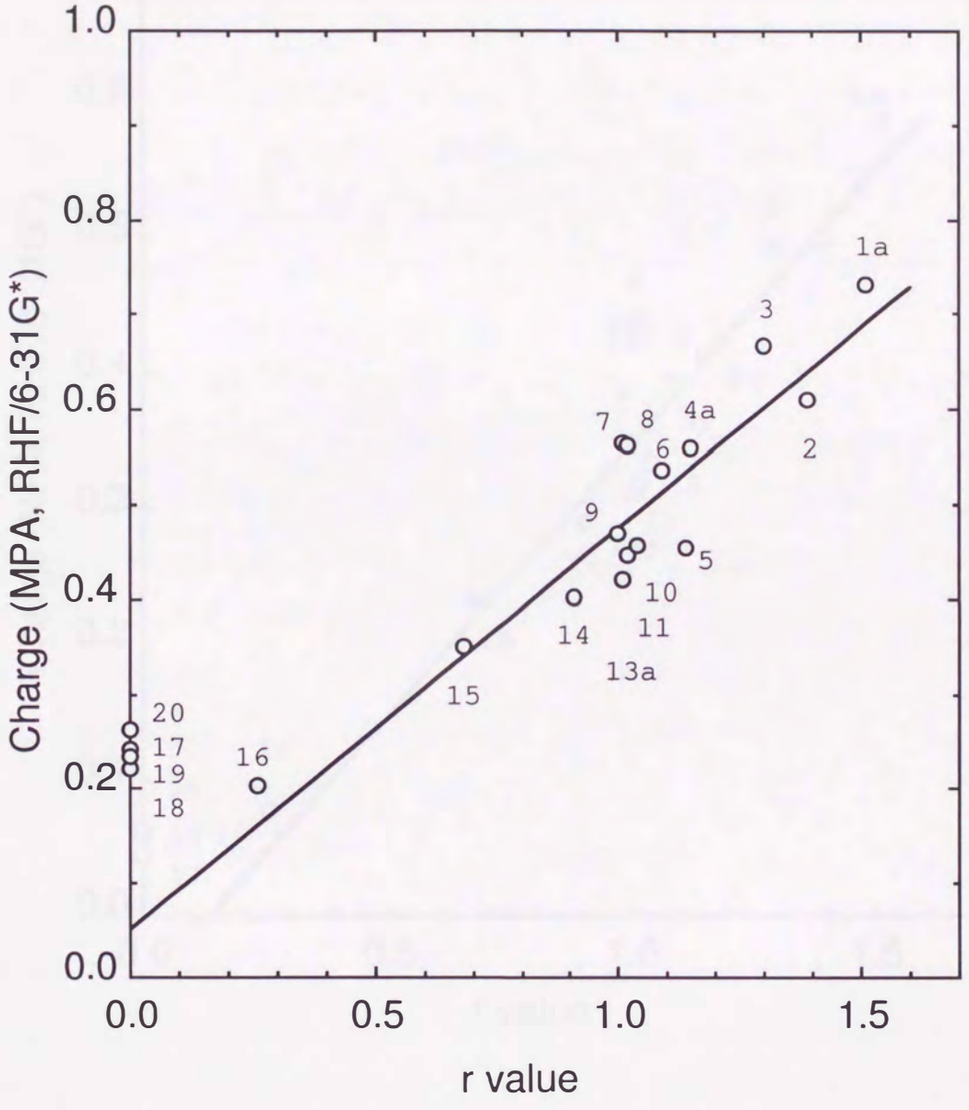

Fig. 4-18. Sum of Mulliken population on phenyl ring (RHF/6-31G*) vs r values in Yukawa-Tsuno equation for benzylic cations. Numbers correspond to those for species in Figs. 4-1 and 4-2.

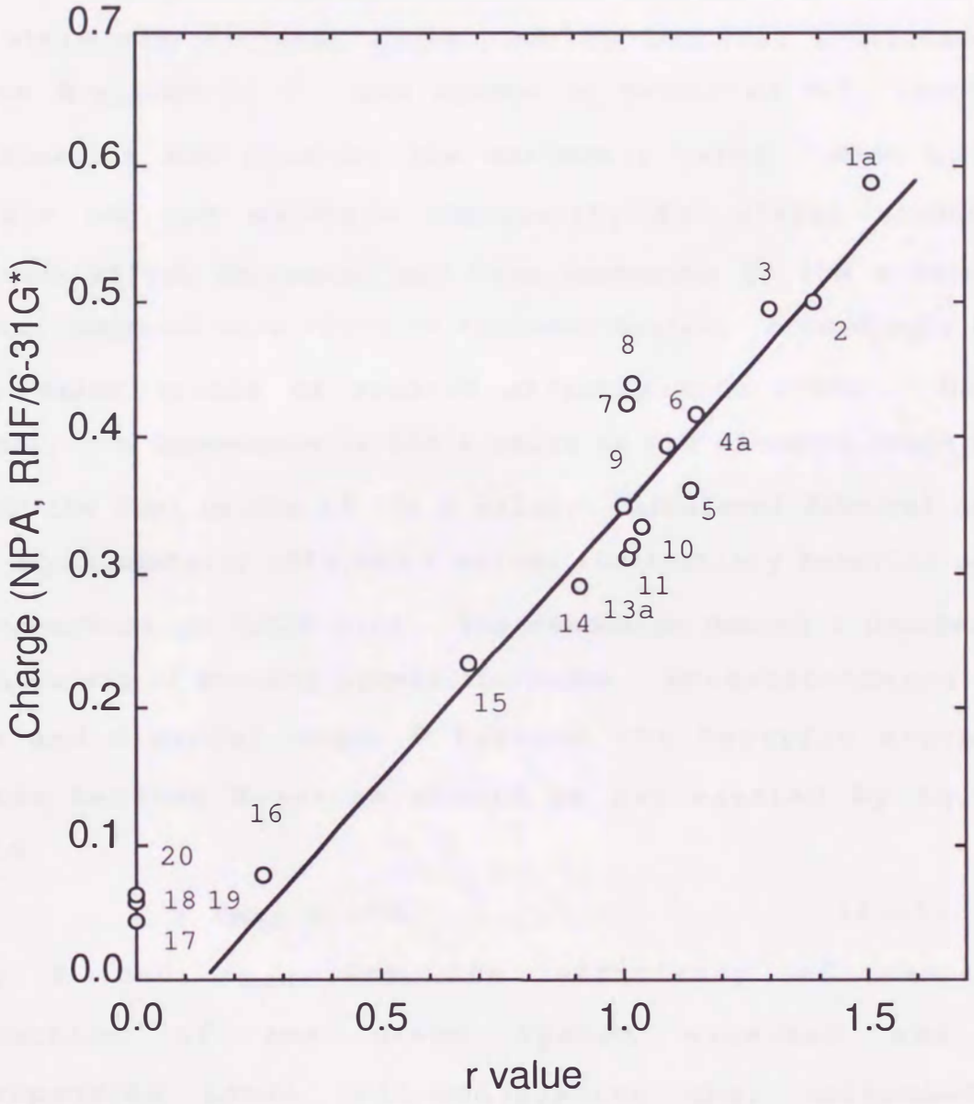

Fig. 4-19. Sum of Natural population on phenyl ring (RHF/6-31G*) vs r values in Yukawa-Tsuno equation for benzylic cations. Numbers correspond to those for species in Figs. 4-1 and 4-2.

related most closely to the degree of π-overlapping between the aryl π-orbital and benzylic p-orbital in the carbocation. In the case where the dihedral angle made by benzylic p-orbital and benzene π-system is 0°, the system is permitted full resonance stabilization and provides the maximum r value. When both p-orbitals can not maintain coplanarity for steric hindrance, resonance effect decreases and then decreases in the r value is observed compared with those of coplanar system. Accordingly θ and the r value should be related strictly each other. On the contrary, the dependence of the r value on the dihedral angle θ may provide the real origin of the r value. Calculated dihedral angles θ and experimentally obtained r values for tertiary benzylic system are summarized in Table 4-14. The resonance demand r decrease as the bulkiness of α-substituents increases. Interdependence of r value and dihedral angle θ between the benzylic p-orbital and the benzene π-system should be represented by Eq. (4-15).[19]

$$r = r_{max} \cos^2\theta, \qquad (4\text{-}15)$$

where r and r_{max} are the efficiency of resonance interaction of any given system examined and the corresponding ideal full-conjugative one, respectively. Assuming the α-cumyl cation to be a coplanar system (θ=0°) in addition to the similarity of electronic effect of α-alkyl groups on the r value, the r value of α-cumyl cation may be regarded as a reference r_{max} value of a coplanar tertiary carbocation. According to Eq. (4-15), the

Table 4-14. Calculated Torsion Angles (in unit of θ[a]) between Alkyl Groups and Benzene Ring for Some Tertiary Benzylic Cations and the Comparison with the Experimental Data.

species	θ_{calc}				r_{sol}[c]	θ_{sol}[d]	r_{gas}[e]	θ_{gas}[f]
	RHF/ STO-3G	RHF/ 3-21G	RHF/ 6-31G*	MP2/ 6-31G*// RHF/ 6-31G*[b]				
9	0	5	5	4.3	1.00	0	1.00[k]	0
10	2	2	3		1.04[g]	0	1.01[l]	0
11	1	1	0		1.02[h]	0		
13a	10	11	10		1.01[g]	0		
14	20	24	24	23.8	0.91[i]	17	0.86[m]	22
15	31	37	33		0.68[h]	34		
16	55	77	76	71.0	0.26[j]	59		
17	90	90	90		0	90		

a) See Fig. 4-3. b) Given by 6-31G*+MP2. See text. c) r value given in Yukawa-Tsuno substituent effect analysis for the solvolysis of each system. d) $r_{sol}/r_{solmax} = \cos^2\theta_{sol}$. e) r value given in Yukawa-Tsuno substituent effect analysis for the gas phase stabilities of each system. f) $r_{gas}/r_{gasmax}=\cos^2\theta_{gas}$. g) Ref. 3h. h) Unpublished results in this laboratory. i) Ref. 3i. j) Ref. 3j. k) Ref. 4f. l) Ref. 4e. m) Ref. 4g.

torsional angle between vacant p-orbital and benzene π-system of tertiary cations are estimated as shown in Table 4-14. Torsional angles θ in solvolysis and gas phase cation agree with each other supporting intrinsically identical structure between transition state and corresponding cation (see chapter 3). As shown in Fig. 4-20, a good correlation exists, between theoretically calculated θ_{calc} at RHF/6-31G* and experimentally estimated θ_{sol} for tert. benzylic cations. The important thing in the MO calculation is whether the level of theory and basis set are satisfactory to describe the phenomena or not. Especially orbital interaction becomes important in the congested systems. One may suggest that electron correlation must be taken into account for such species. Unfortunately geometry optimization at MP2 or higher level of theories can not be performed for these bulky systems because of the limitation of the hardware. Thus, in order to discuss the effect of electron correlation on the torsion angle θ, single point calculation at MP2 level about **9**, **14**, and **16** were carried out with the geometry where dihedral angle θ changes ±5° around C_1-C_7 axis from the RHF/6-31G* optimized geometry. Energy difference between the structure of each dihedral angle and equilibrium one are plotted in Fig. 4-21. The abscissa is additional angle from the equilibrium θ. The plots of all cations are correlated in second order functions. For **9** and **14**, correlation curve is also symmetrical to both sides of the

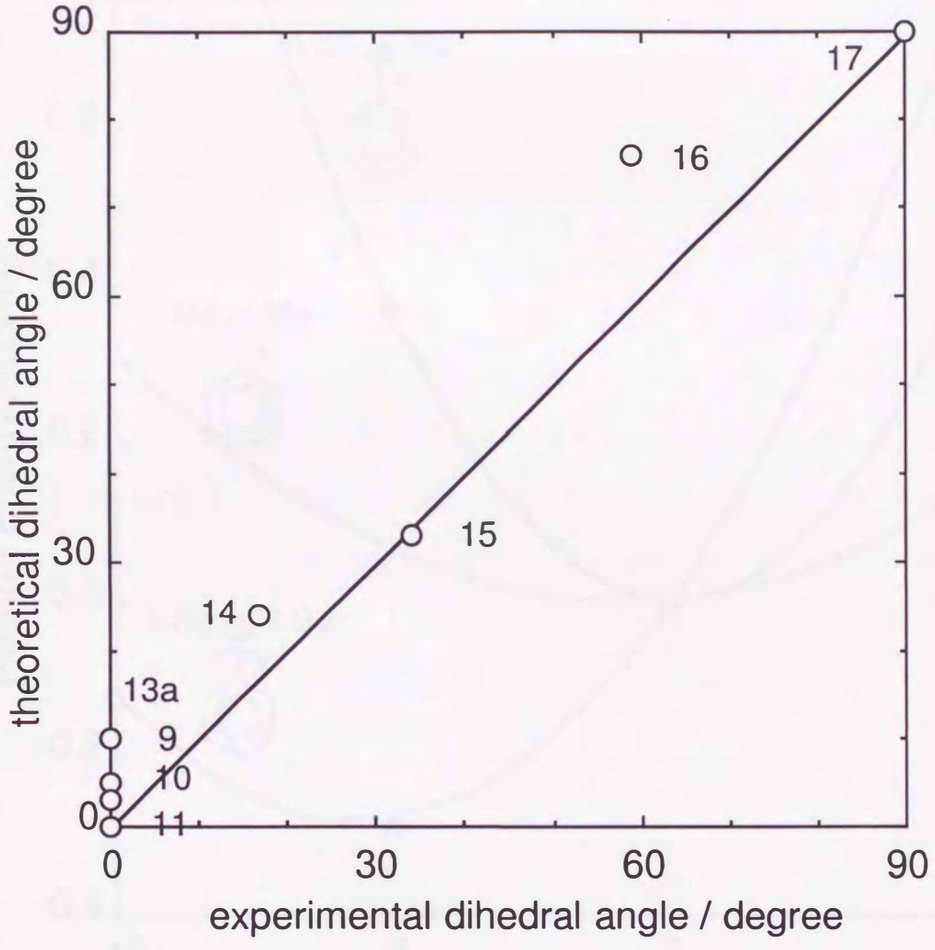

Fig. 4-20. Calculated dihedral angle θ (refer to Figure 4-1) at RHF/6-31G* vs. torsion angle θ estimated by $r/r_{max}=\cos^2\theta$, where r is the resonance demand in Yukawa-Tsuno equation obtained from solvolysis of the corresponding precursors. Numbers correspond to those for species in Figs. 4-1 and 4-2.

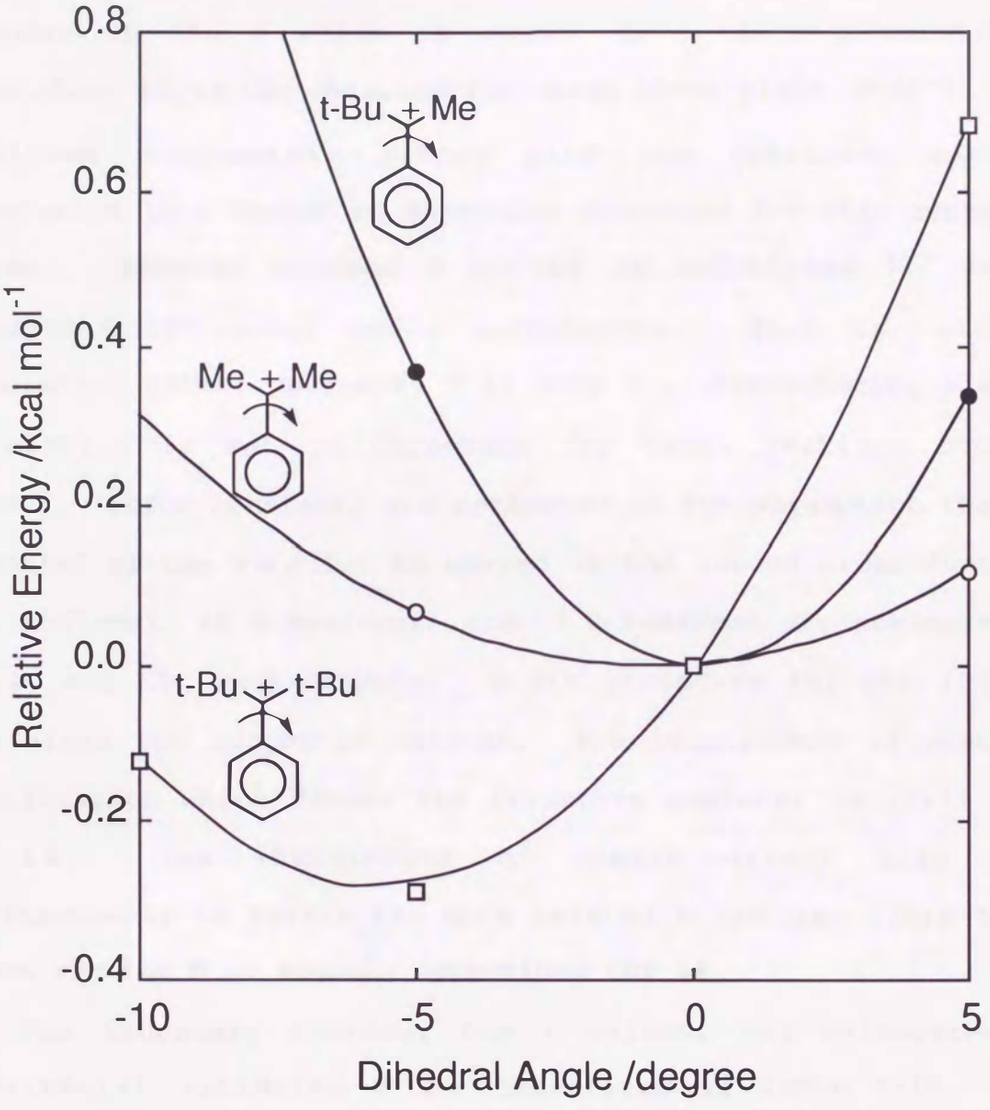

Fig. 4-21. Fixed dihedral angle vs. energy for α,α-dimethylbenzyl (open circle), α-*t*-buthyl-α-methylbenzyl (closed circle), and α,α-di-*t*-butylbenzyl (open square) cations.

equilibrium θ at RHF/6-31G*; electron correlation does not affect the optimized structure. For **16**, single point calculation was extended to the θ which is swung -10°, since a monotonical correlation curve was obtained for these three plots (θ=±5°). As a resulting unsymmetric curved plot was obtained; electron correlation is a factor to determine structure for this conjugated system. However minimum θ for **16** is calculated 71° in the assumption of second order correlation. That is, electron correlation effect decreases θ in only 5°. Consequently electron correlation is not so important for these tertiary benzylic cations. Force constants are estimated in the assumption that the potential of the rotation is obeyed in the second order function. 7.35 kcal/mol, 28.5 kcal/mol, and 17.0 kcal/mol are estimated for **9**, **14**, and **16**, respectively. Rigid structure for the rotation were given for congested cations. The requirement of resonance stabilization which forces the structure coplanar is still large for **14**. The requirement of steric effect also exist simultaneously to rotate the more twisted structure. This is the reason why the θ is rigidly determined for **14**.

For secondary systems, the r values, and calculated and experimental estimated θ are summarized in Table 4-15. 2,2-Dimethyl-1-indanyl system (**5**) is assumed to a coplanar standard of secondary system. The values do not change drastically compared to those for tert. systems as shown in Table 4-15. This may be attributed intrinsically to the large resonance demand of secondary systems. θ_{obs} and θ_{calc} are fairly agree with each other. This

Table 4-15. Calculated Torsion Angles (in unit of θ[a]) between Alkyl Groups and Benzene Ring for Some Secondary Benzylic Cations and the Comparison with the Experimental Data.

species	θ_{calc}			r_{sol}[b]	θ_{sol}[c]
	RHF/ STO-3G	RHF/ 3-21G	RHF/ 6-31G*		
5	0	0	0	1.11[d]	0
4a			0	1.15[e]	0
6	0	0	0	1.09[f]	8
7	0	0	0	1.01[g]	17
8	16	25	22	1.02[g]	17

a) See Fig. 4-3. b) r value given in Yukawa-Tsuno substituent effect analysis for the solvolysis of each system. c) $r_{sol}/r_{solmax} = \cos^2\theta_{sol}$. d) Ref. 3g. e) Ref. 3d. f) Ref. 3e. g) Ref. 3f.

supports that the r value is the parameter indicating the resonance degree.

Conclusion

The ab initio MO calculations of some benzylic cations were performed, since the transition state structures of S_N1 benzylic solvolysis can be approximated to the parent cation (see chapter 3). All indices (rotational barrier, bond length, bond order, and charge distribution) are well correlated to the empirical r value from Yukawa-Tsuno substituent effect analysis. The relation of each theoretical index and the r value is completely agreed with

the prediction by the resonance theory. This provides theoretical support that the r value is the real parameter indicating the degree of resonance interaction between benzylic p-orbital and benzene π-system. In both sec. and tert. systems, calculated dihedral angle θ can be related to corresponding θ experimentally obtained by the equation of $r = r_{max} \cos^2\theta$ from solvolysis reactivity and cation stability. This also support the evidence concerning the origin of the r value.

References

1) Y. Yukawa and Y. Tsuno, *Bull. Chem. Soc. Jpn.*, **32**, 971 (1959); Y. Yukawa, Y. Tsuno, and M. Sawada, *Bull. Chem. Soc. Jpn.*, **39**, 2274 (1966).

2) a) A. Murata, M. Goto, R. Fujiyama, M. Mishima, M. Fujio, and Y. Tsuno, *Bull. Chem. Soc. Jpn.*, **63**, 1129 (1990). b) A. Murata, S. Sakaguchi, R. Fujiyama, M. Fujio, and Y. Tsuno, *Bull. Chem. Soc. Jpn.*, **63**, 1138 (1990). c) M. Fujio, M. Goto, T. Susuki, I. Akasaka, M. Mishima, and Y. Tsuno, *Bull. Chem. Soc. Jpn.*, **63**, 1146 (1990); M. Fujio, M. Goto, T. Susuki, M. Mishima, and Y. Tsuno, *J. Phys. Org. Chem.*, **3**, 449 (1990). d) Y. Tsuno, Y. Kusuyama, M. Sawada, T. Fujii, and Y. Yukawa, *Bull. Chem. Soc. Jpn.*, **48**, 3337 (1975); M. Fujio, T. Adachi, Y. Shibuya, A. Murata, and Y. Tsuno, *Tetrahedron Lett.*, **25**, 4557 (1984). e) Y. Tsuji, M. Fujio, and Y. Tsuno, *Bull. Chem. Soc. Jpn.*, **63**, 856 (1990). f) M. Fujio, Y. Tsuji, T. Otsu, and Y. Tsuno, *Tetrahedron Lett.*, **32**, 1805 (1991). g) M. Fujio, K. Nakata, Y. Tsuji, T. Otsu, and Y. Tsuno, *Tetrahedron Lett.*, **33**, 321 (1992). h) M. Fujio, K. Nakata, T. Kuwamura, H. Nakamura, Y. Saeki, M. Mishima, S. Kobayashi, and Y. Tsuno, *Tetrahedron Lett.*, **34**, 8309 (1993). i) M. Fujio, H. Nomura, K. Nakata, Y. Saeki, M. Mishima, S. Kobayashi, T. Matsushita, K. Nishimoto, and Y. Tsuno, *Tetrahedron Lett.*, **35**, 5005 (1994).

j) M. Fujio, T. Miyamoto, Y. Tsuji, and Y. Tsuno, *Tetrahedron Lett.*, **32**, 2929 (1991). k) M. Fujio, K. Nakashima, E. Tokunaga, Y. Tsuji, and Y. Tsuno, *Tetrahedron Lett.*, **33**, 345 (1992).

3) a) M. Mishima, H. Inoue, M. Fujio, and Y. Tsuno, *Tetrahedron Lett.*, **30**, 2101 (1989). b) M. Mishima, H. Inoue, M. Fujio, and Y. Tsuno, *Tetrahedron Lett.*, **31**, 685 (1990). c) M. Mishima, K. Arima, S. Usui, M. Fujio, and Y. Tsuno, *Mem. Fac. Sci., Kyushu Univ., Ser. C*, **15(2)**, 277 (1986); M. Mishima, K. Arima, S. Usui, M. Fujio, and Y. Tsuno, *Chem. Lett.*, **1987**, 1047. d) M. Mishima, S. Usui, M. Fujio, and Y. Tsuno, *Nippon Kagaku Kaishi*, **1989**, 1269. e) M. Mishima, H. Nakamura, K. Nakata, M. Fujio, and Y. Tsuno, *Chem. Lett.*, **1994**, 1607. f) M. Mishima, S. Usui, H. Inoue, M. Fujio, and Y. Tsuno, *Nippon Kagaku Kaishi*, **1989**, 1262. g) M. Mishima, K. Nakata, H. Nomura, M. Fujio, and Y. Tsuno, *Chem. Lett.*, **1992**, 2435; K. Nakata, H. Nomura, M. Mishima, Y. Saeki, K. Nishimoto, T. Matsushita, M. Fujio, and Y. Tsuno, *Mem. Fac. Sci., Kyushu Univ., Ser. C*, **18(2)**, 287 (1992).

4) W. J. Hehre, L. Radom, P. v. R. Schleyer, and J. A. Pople, *Ab initio Molecular Orbital Theory*; Wiley: New York (1986).

5) M. J. Frisch, G. W. Trucks, M. Head-Gordon, P. M. W. Gill, M. W. Wong, J. B. Foresman, B. G. Johnson, H. B. Schlegel, M. A. Robb, E. S. Replogle, R. Gemperts, J. L. Andres, K. Raghavachari, J. S. Binkley, C. Gonzalez, R. L. Martin, D. J. Fox, D. J. DeFrees, J. Baker, J. J. P. Stewart, and J. A. Pople, GAUSSIAN 92; Gaussian Inc.: Pittsburgh, PA (1992)

6) H. B. Schlegel, *J. Comput. Chem.*, **7**, 359 (1986).

7) C. Møller and M. S. Plesset, *Phys. Rev.*, **46**, 618 (1934).

8) J. A. Pople, H. B. Schlegel, R. Krishnan, D. J. DeFrees, J. S. Binkley, M. J. Frisch, R. A. Whiteside, R. F. Hout, and W. J. Hehre, *Int. J. Quantum Chem. Symp.*, **15**, 269 (1981); D. J. DeFrees and A. D. McLean, *J. Chem. Phys.*, **82**, 33 (1985).

9) A. E. Reed, R. B. Weinstock, and F. Weinhold, *J. Chem. Phys.*, **83**, 735 (1985); A. E. Reed, L. A. Curtiss, and F. Weinhold,

Chem. Rev., **88**, 899 (1988); J. E. Carpenter and F. J. Weinhold, *J. Mol. Struct.*, **169**, 41 (1988).

10) R. S. Mulliken, *J. Chem. Phys.*, **23**, 1833 (1955).

11) W. J. Hehre, M. Taagepera, R. W. Taft, and R. D. Topsom, *J. Am. Chem. Soc.*, **103**, 1344 (1981).

12) A. E. Dorigo, Y. Li, and K. N. Houk, *J. Am. Chem. Soc.*, **111**, 6942 (1989).

13) K. Raghavachari, R. A. Whiteside, J. A. Pople, and P. v. R. Scleyer, *J. Am. Chem. Soc.*, **103**, 5649 (1981).

14) H. Mayr, W. Forner, and P. v. R. Schleyer, *J. Am. Chem. Soc.*, **101**, 6032 (1979).

15) K. B. Wieberg, *Tetrahedron*, **24**, 1083 (1968).

16) C. A. Coulson, *Proc. R. Soc. A*, **169**, 413 (1939); C. A. Coulson, *J. Phys. Chem.*, **56**, 311 (1952).

17) J. M. Martin, M. Fernandez, and J. Tortajada, *J. Mol. Struct.*, **175**, 203 (1988).

18) For a review , see: S. M. Bachrach, *Reviews in Computational Chemistry Vol. V, Chap. 3*; K. B. Lipkowitz and D. B. Boyd, Eds; VCH: Germany (1993).

19) P. B. D. de la Mare, E. A. Johnson, and J. S. Lomas, *J. Chem. Soc.*, **1964**, 5317; K. Ohkata, R. L. Paquette, and L. A. Paquette, *J. Am. Chem. Soc.*, **101**, 6687 (1979) ; J. M. Tanko, N. Kamrudin, and J. F. Blackert, *J. Org. Chem.*, **56**, 6395 (1991).

Materials:

Preparation of 5- and 6-Substituted Indan-1-ones:

5-MeS, 5-PhO, 6-Me, 6-Cl, and 6-Br indan-1-ones were prepared by Friedel-Crafts ring closure of the corresponding 3-arylpropionyl chlorides.[1] 5-MeO-6-Cl, 5,6-Me_2, 5-Me, 5-*t*-Bu, and 5-Br derivatives were obtained from the corresponding 3-chloropropiophenones according to Adamczyk's method.[2] Other substituted indan-1-ones were commercially available. Physical constants and analytical data of 2,2-dimethylindan-1-ols were summarized in Tables 5-1 and 5-2.

Preparation of 5- and 6-Substituted 2,2-Dimethylindan-1-ones:

The above ketone was methylated to α,α-dimethyl derivatives according to Roberts's method[3] . Under nitrogen atmosphere, DMSO (2.2 equiv) was added to sodium hydride. A solution of 5 or 6-substituted indan-1-one and CH_3I (2 equiv) in THF-DMSO was added to the above mixture slowly so as to maintain at 20-35°C. The resultant thick slurry was stirred for 6h, left overnight, and water was added dropwise. The mixture was extracted with ether, washed with saturated brine, and dried over anhydrous magnesium sulfate. Crude product was purified by medium pressure liquid chromatography on Merck Lichroprep Si60 with 1:10 AcOEt-hexane. Physical constants were listed in Table 5-1.

Table 5-1. Physical Constants[a] of Substituted Indan-1-ones, 2,2-Dimethylindan-1-ones, 2,2-Dimethylindan-1-ols, and 2,2-Dimethylindan-1-yl Chlorides

Substituent	Indan-1-ones	2,2-Dimethyl-indan-1-ones	2,2-Dimethyl-indan-1-ols	2,2-Dimethyl-indan-1-yl Cl
	-mp/°C-			
5-MeO			103.0-103.8	
5-MeS			84.5-85.0	47.0-49.0
5-PhO			80.0-81.0	
5-MeO-6-Cl	144.0-145.0	99.5-100.2	153.0-154.8	83.0-86.0
5,6-Me_2	84.0-86.5		81.0-81.7	
5-Me	69.5-71.0		48.0-48.3	
5-*t*-Bu			82.6-83.0	
6-Me	59.4-61.2		45.7-46.6	
H			55.0-55.5(56-57)[b]	
6-MeO			67.6-68.2	
5-Br			65.0-65.8	
6-Cl	75.6-77.6		100.1-100.9	
6-Br	109.4-110.4(109-110)[c]		98.3-99.1	
6-CN			73.0-74.2	30-33
5-CN		93.7-94.3	73.6-74.3	49.3-50.3

a) Uncorrected melting points. b) Ref. 4. c) Ref. 2.

Table 5-2. Analytical Data of 2,2-Dimethylindan-1-ols

Substituent	Carbon/%		Hydrogen/%		Nitrogen/%	
	Calcd	Found	Calcd	Found	Calcd	Found
5-MeO	74.97	74.91	8.39	8.45		
5-MeS	69.19	69.32	7.74	7.78		
5-PhO	80.26	80.10	7.13	7.15		
5-MeO-6-Cl	63.58	63.59	6.67	6.66		
5,6-Me_2	82.06	81.94	9.54	9.39		
5-Me	81.59	81.77	9.12	9.15		
5-*t*-Bu	82.52	82.48	10.16	10.21		
6-Me	81.77	81.74	9.15	9.10		
H	81.44	81.41	8.70	8.72		
6-MeO	74.97	74.96	8.39	8.40		
5-Br	54.79	54.57	5.43	5.44		
6-Cl	67.18	67.16	6.66	6.57		
6-Br	54.79	54.81	5.43	5.46		
6-CN	76.98	77.15	7.00	7.07	7.48	7.48
5-CN	76.98	76.82	7.00	6.98	7.48	7.46

Preparation of 5- and 6-Cyano-2,2-dimethylindan-1-one:

A mixture of 5- (or 6-)bromo-2,2-dimethylindan-1-one and copper(I) cyanide (1.36 equiv) in DMF was refluxed for 5h. The reaction mixture was poured into a solution of $FeCl_3 \cdot 6H_2O$ and hydrochloric acid in water, heated for 30min at 55-60°C, and then cooled for 1h at 0°C. The solution was extracted with benzene, washed with brine, and dried over anhydrous magnesium sulfate. Crude product was purified by the silica gel chromatography to afford 5-cyano-2,2-dimethylindan-1-one, and recrystallized from benzene-hexane.

Preparation of 5- and 6-Substituted 2,2-Dimethylindan-1-ols:

To $NaBH_4$ (20 equiv) was added a solution of aqueous NaOH solution (1N) in methanol, and then a solution of 5 or 6-substituted 2,2-dimethylindan-1-one in methanol at 0°C. After stirring for 5h, the product was poured into water, extracted with ether, washed with brine, and dried over anhydrous magnesium sulfate. The crude product obtained by evaporation of the solvent was recrystallized from hexane. Physical constants and analytical data were summarized in Tables 5-1 and 5-2.

Preparation of 5- and 6-Substituted 2,2-Dimethylindan-1-yl chlorides:

To a solution of 5 or 6-substituted 2,2-dimethylindan-1-ol in ether in the presence of anhydrous $CaCl_2$ was bubbled dry hydrogen chloride at 0°C for 4h. The reaction mixture was filtered after drying with anhydrous magnesium sulfate, and the solvent was removed under reduced pressure. This procedure was repeated till

excess HCl was completely removed. For 5-CN and 6-CN derivatives, $ZnCl_2$ was used as catalyst with dry hydrogen chloride. Physical constants were summarized in Table 5-1.

Preparation of 2-aryl-3,3-dimethylbutan-2-ols:[5)]

To stirred solution of commercial n-butyllithium (0.1 mol, 1 equiv) in hexane was added a solution of 3- or 4-substituted bromobenzene (1 equiv) in ether under N_2 atmosphere at -50°C. Then the mixture was stirred for 1h at room temperature. To the reaction mixture was added a solution of pinacolone (1 equiv) in ether at -30°C. Then the mixture was stirred overnight. The reaction mixture was poured into a solution of ammonium chloride in water, extracted with ether, washed with saturated brine, and dried over anhydrous magnesium sulfate. The solvent was removed to give the crude product which was purified by chromatograph on SiO_2 (Merck, Lichroprep.Si60) with hexane-AcOEt 10:1. Physical constants were summarized in Table 5-3.

Preparation of 2-aryl-3,3-dimethyl-1-butenes:[6)]

2-(3- or 4-substituted phenyl)-3,3-dimethylbutan-2-ol was passed over activated alumina at 275°C, under reduced pressure (40mmHg) for 1h. The product was dried with anhydrous magnesium sulfate in ether. The crude olefin was obtained by evaporation of solvent, and was purified by chromatograph on SiO_2 (Merck, Lichroprep.Si60) with hexane. Analytical data were summarized in Table 5-4.

Table 5-3. Physical Constants[a] of 2-Aryl-3,3-dimethylbutan-2-ols.

Substituent	2-Aryl-3,3-dimethyl-butan-2-ols -mp °C (or bp °C/mmHg)-
p-MeS	41.9-42.6
m,m-Me_2	(88-91°C/0.5mmHg)
m-F	(75-76°C/0.9mmHg)
m-CF_3	30.5-31.2
p-CF_3	(109-111°C/9mmHg)

a) Uncorrected melting points.

Table 5-4. Analytical Data of 2-Aryl-3,3-dimethyl-1-butene.

Substituent	Carbon %		Hydrogen %	
	Calcd	Found	Calcd	Found
p-MeO	82.06	81.88	9.53	9.45
p-MeS	75.67	75.82	8.79	8.82
p-MeO-m-Cl	69.48	69.28	7.63	7.53
p-Me	89.51	89.48	10.41	10.29
3,5-Me_2	89.29	89.28	10.71	10.77
m-Me	89.51	89.75	10.41	10.44
H	89.94	89.69	10.06	9.95
m-Cl	74.03	73.83	7.77	7.72
m-F	80.86	80.95	8.48	8.47
m-CF_3	68.41	68.28	6.62	6.61
p-CF_3	68.41	68.22	6.62	6.68

Solvents[7)]

Commercial acetone was refluxed with $KMnO_4$ for 6h and distilled. The distillate was dried over anhydrous Na_2CO_3 for three days and fractionated. Aqueous organic solvents (90%, 80%, and 50% v/v acetone) were prepared by mixing the corresponding volumes of water and acetone at 25°C.

Measurements

Kinetic measurements:[8)]

Solvolysis rates in aqueous acetone were followed conductometrically. Conductance measurements were made in a cell with bright platinum electrodes using approximately 25 or 50 ml of 10^{-4} - 10^{-5} M solution of a starting chloride. Conductance readings were taken by using a conductivity meter (CM50AT and CM60S equipped with interval unit and printer, Toa Electronics Ltd.). Solvolysis reactions were followed by taking at least 100 readings at an appropriate interval for 2.5 half-lives, and the infinity reading was taken after 10 half-lives. The solvolysis rates for less reactive substrates were followed at high temperature by using the ampoule technique with conductivity determination. The conductance readings were then fitted to the first-order rate equation by means of least-squares computer program; the precision of fit to first-order kinetics was generally satisfactory over 2.5 half-lives ($R>0.99998$).

Gas Phase Basicity Measurement:[9)]

The gas phase basicity measurement was performed with a pulsed ion cyclotron resonance (ICR) mass spectrometer.

The equilibrium constant K for a proton transfer reaction (5-1),

(5-1)

is given by

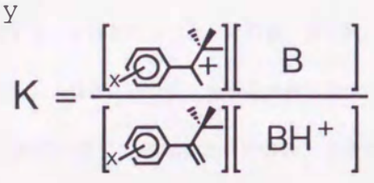

(5-2)

where B is the reference base of known basicity (Table 5-5). The standard free energy change for this reaction is obtained by

$$\Delta G^{o} = -RT \ln K. \qquad (5\text{-}3)$$

All samples were purified by vapor phase chromatography

Table 5-5. Reference Base for Determining Basicities of α-*t*-Butylstyrene

Base B	ΔGB / kcal mol^{-1}	Base B	ΔGB / kcal mol^{-1}
CH_3CONMe_2	12.8	Acetylacetone	3.7
3-Cl-pyridine	11.5	i-Pr_2O	2.0
2-Cl-pyridine	11.0	c-PrCOMe	0.7
p-$CH_3C_6H_4NH_2$	10.1	n-Pr_2O	-1.7
$(MeO)_3PO$	9.3	tBuMeCO	-2.0
2-F-pyridine	7.4	Et_2CO	-2.8
$C_6H_5NH_2$	6.9	AcOEt	-3.6
4-CN-pyridine	6.5	Et_2O	-3.9
3-CN-pyridine	5.7	$(MeO)_2CO$	-4.2
		THF	-5.2

a) Relative to ammonia. (GB of NH_3 = 195.6 kcal mol^{-1})

and by bulb to bulb transfer in vacuum line immediately before use. The inlet system and the ICR analyzer were warmed to 70°C with resistance heating tapes. An experiment is initiated by a 10 ms pulse of an electron beam (20 eV) through the ICR cell. After a certain period of reaction, detect pulse is triggered and the capacitance bridge detector measures the abundance of the ions. By slowly varying the delay time of the detect pulse, a "time plot" of ion abundance against reaction time was recorded. The relative equilibrium abundance of α-*t*-butyl-α-methylbenzyl cation and BH^+ was given by the relative ion signal intensity at steady state after an initial reaction period of about 400 to 1500 ms. In order to avoid artifacts caused by ion loss, an experiment was carried out at a constant magnetic field strength (12kG) where the rates of ion loss were expected to be comparable for two ions with different mass. The pressure of the neutral reactants was measured by means of a Bayard-Alpert ionization gauge with appropriate correction factors being applied to correct gauge reading for the different ionization cross sections of the various compounds. Several measurements were carried out for each sample by using at least two different reference bases. The free energy changes for respective proton transfer reactions are summarized in Table 5-6. The uncertainty in the gas phase basicities is estimated to be within ±0.2kcal/mol.

Table 5-6. Standard Free Energy Changes of Proton Transfer Equilibria

α-*t*-Butylstyrene Subst.	Reference base B	ΔG^{o} [a] /kcal mol^{-1}	Selected ΔGB [b] /kcal mol^{-1}
p-MeO	CH_3CONMe_2	+1.4	11.0
	3-Cl-pyridine	+0.8	
	2-Cl-pyridine	0.0	
p-MeS	2-Cl-pyridine	+1.0	10.5
	p-$CH_3C_6H_4NH_2$	-0.7	
	$(MeO)_3PO$	-1.3	
p-MeO-m-Cl	2-F-pyridine	-0.6	7.9
	$C_6H_5NH_2$	-0.8	
p-Me	4-CN-pyridine	+0.5	6.0
	3-CN-pyridine	-0.2	
3.5-Me_2	3-CN-pyridine	-0.3	6.0
	Acetylacetone	-2.3	
m-Me	Acetylacetone	-0.9	4.4
	i-Pr_2O	-2.2	
H	Acetylacetone	+1.1	2.4
	i-Pr_2O	-0.3	
	c-PrCOMe	-1.8	
m-Cl	n-Pr_2O	0.0	-1.9
	Et_2CO	-0.9	
	AcOEt	-1.8	
m-F	Et_2CO	-0.7	-2.3
	AcOEt	-1.4	
m-CF_3	n-Pr_2O	+2.2	-3.6
	Et_2O	-0.4	
p-CF_3	$(MeO)_2CO$	+0.7	-4.8
	THF	-0.5	

a) Free energy changes for reaction (5-1) at 343K. b) Relative to ammonia.

References

1) F. Mayer and P. Müller, *Ber.*, **60**, 2278 (1927).

2) M. Adamczyk and D. S. Watt, *J. Org. Chem.*, **49**, 4226 (1984).

3) D. D. Roberts, *J. Org. Chem.*, **39**, 1265 (1974).

4) G. Baddeley, J. W. Rasburn, and R. Rose, *J. Chem. Soc.*, **1958**, 3168.

5) H. Tanida and H. Matsumura, *J. Am. Chem. Soc.*, **95**, 1586 (1973).

6) B. B. Corson, H. E. Tiefenthal, G. R. Atwood, W. J. Heintzelman, and W. L. Reilly, *J. Org. Chem.*, **21**, 584 (1956).

7) S. Usui, Y. Shibuya, T. Adachi, M. Fujio, and Y. Tsuno, *Mem. Fac. Sci., Kyushu Univ., Ser. C*, **14(2)**, 355 (1984).

8) M. Fujio, M. Goto, T. Yoshino, K. Funatsu, Y. Tsuji, S. Ouchi, and Y. Tsuno, *Mem. Fac. Sci., Kyushu Univ., Ser. C*, **16(1)**, 85 (1987).

9) M. Mishima, M. Fujio, and Y. Tsuno, *Mem. Fac. Sci., Kyushu Univ., Ser. C*, **14(2)**, 365 (1984).

Acknowledgment

The author would like to express his best gratitude to Professor Yuho Tsuno and Professor Mizue Fujio, whose positive suggestions greatly influenced the direction of this thesis.

The author is sincerely grateful to Professor Kichisuke Nishimoto for his significant discussions and advices concerning ab intio MO calculations.

The author also wishes to appliciate for discussions and technical advices with respect to ICR experiments from Associate Professor Masaaki Mishima

Professor Hans-Ullich Siehl, Associate Professor Nobujiro Shimizu, Associate Professor Shinjiro Kobayashi, Associate Professor Hiroshi Yamataka, Assistant Professor Toshio Matsushita, Dr. Yutaka Tsuji, and Dr. Yoshihiro Saeki are acknowledged for their many useful suggestions and continuous encouragements.

Finally, the author thanks Mr. Katsuo Token, Dr. Satoshi Usui, Dr. Song-Hong Kim, Dr. Yoshiyuki Kuwatani, and other staffs and students of Institute for Fundamental Research of Organic Chemistry for their cooperations.

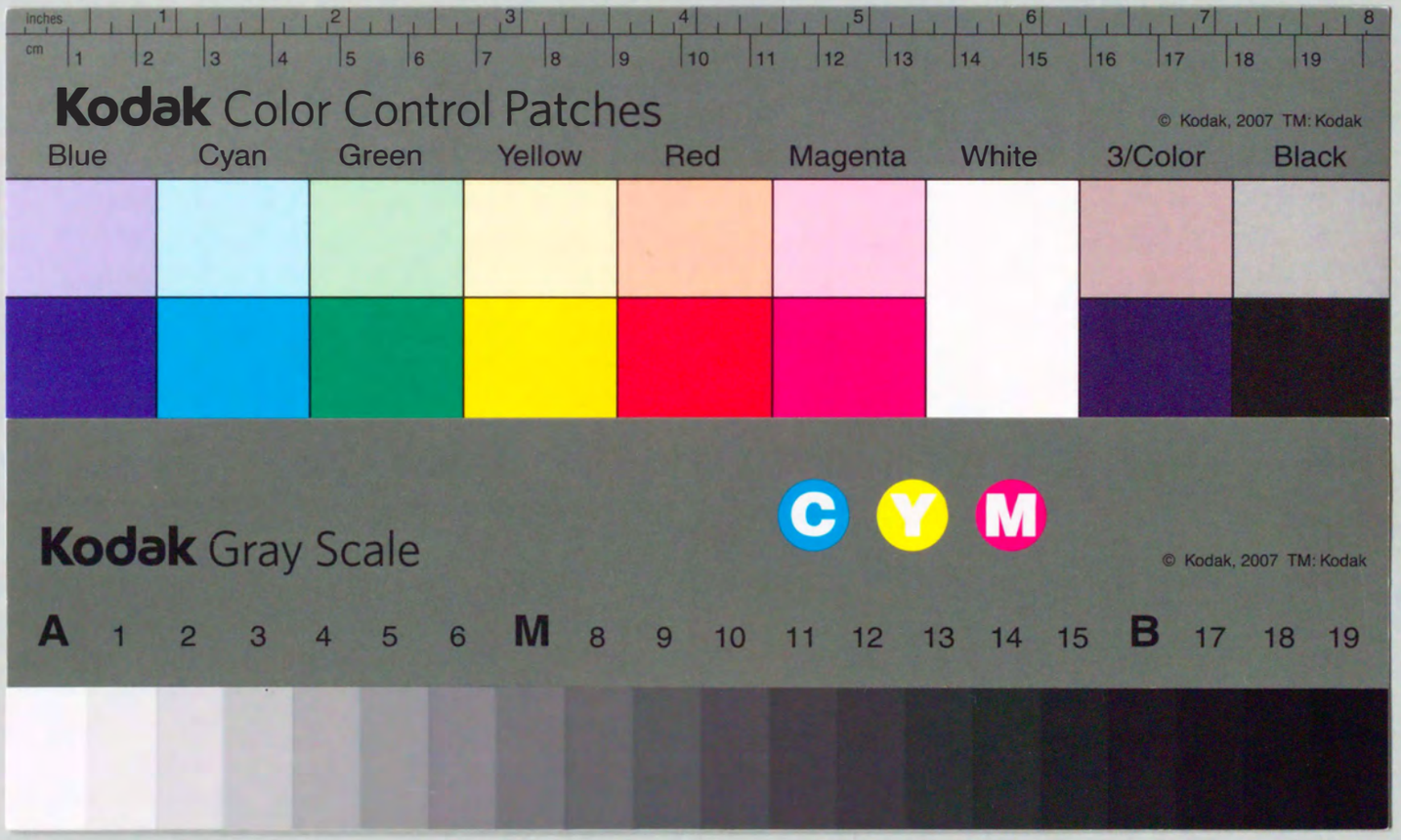
inches
cm
Kodak Color Control Patches
© Kodak, 2007 TM: Kodak
Blue
Cyan
Green
Yellow
Red
Magenta
White
3/Color
Black
Kodak Gray Scale
C
Y
M
© Kodak, 2007 TM: Kodak
A 1 2 3 4 5 6 M 8 9 10 11 12 13 14 15 B 17 18 19